

Equations for Estimating Horizontal Response Spectra and Peak Acceleration from Western North American Earthquakes: A Summary of Recent Work

David M. Boore, William B. Joyner, and Thomas E. Fumal

U.S. Geological Survey, Menlo Park, California

ABSTRACT

In this paper we summarize our recently-published work on estimating horizontal response spectra and peak acceleration for shallow earthquakes in western North America. Although none of the sets of coefficients given here for the equations are new, for the convenience of the reader and in keeping with the style of this special issue, we provide tables for estimating random horizontal-component peak acceleration and 5 percent damped pseudo-acceleration response spectra in terms of the natural, rather than common, logarithm of the ground-motion parameter. The equations give ground motion in terms of moment magnitude, distance, and site conditions for strike-slip, reverse-slip, or unspecified faulting mechanisms. Site conditions are represented by the shear velocity averaged over the upper 30 m, and recommended values of average shear velocity are given for typical rock and soil sites and for site categories used in the National Earthquake Hazards Reduction Program's recommended seismic code provisions. In addition, we stipulate more restrictive ranges of magnitude and distance for the use of our equations than in our previous publications. Finally, we provide tables of input parameters that include a few corrections to site classifications and earthquake magnitude (the corrections made a small enough difference in the ground-motion predictions that we chose not to change the coefficients of the prediction equations).

INTRODUCTION

The design of any engineered structure is based on an estimate of ground motion, either implicitly through the use of building codes or explicitly in the site-specific design of large or particularly critical structures. Rarely are there a sufficient number of ground-motion recordings near a site to allow a direct empirical estimation of the motions expected for a design earthquake. It is therefore necessary to develop relationships, expressed in the form of equations or graphical

curves, for estimating ground motions in terms of magnitude, distance, site conditions, and other variables from the body of strong-motion data from a large region or a particular tectonic setting. This is so for site-specific design as well as for regional hazard mapping.

Our first equations for estimating horizontal response spectra and peak acceleration were developed from strong-motion data recorded before 1981 in western North America (Joyner and Boore, 1981, 1982); we will refer to these first studies as "JB8182." We are engaged in a long-term effort to revise those equations, incorporating new data and extending the period range covered by the equations, which will require reprocessing all of the data. Pending completion of this work, we produced interim equations (Boore *et al.*, 1993), based on the JB8182 data set augmented by data from three large earthquakes in California (1989 Loma Prieta, 1992 Petrolia, and 1992 Landers). These three earthquakes provided data for a range of magnitude and distance which is critical for engineering design and which was poorly represented in the original data set.

The results in Boore *et al.* (1993) were later revised twice. In the first revision (Boore *et al.*, 1994a) the site-effect term was changed from a constant for each site class to a continuous function of shear-wave velocity at the site, averaged to a depth of 30 m. The second revision (Boore *et al.*, 1994b), which was widely distributed but never published, modified the equations to give different ground-motion estimates for strike-slip and reverse-slip earthquakes. The second revision gave equations only for the random horizontal-component of motion for peak acceleration and for 5-percent damped oscillator response; the earlier versions (Boore *et al.*, 1993, 1994a) gave equations for both the random horizontal component and the larger horizontal component for peak acceleration and for oscillator response for damping values of 2, 5, 10, and 20 percent.

For conciseness, we refer to Boore *et al.* (1993), Boore *et al.* (1994a), and Boore *et al.* (1994b) as "BJF93," "BJF94a,"

and "BJF94b," respectively, or as "BJF94ab" or "BJF9394" collectively, as appropriate.

This paper gives a brief description of the equations of BJF93 for peak horizontal acceleration and the random horizontal component for 5 percent damping, incorporating both revisions (BJF94a, BJF94b). More complete information can be found in the BJF9394 publications. We strongly recommend the use of the BJF94ab equations in preference to those of BJF93 because we believe that the BJF94a revision significantly improves the treatment of site effects. In contrast with BJF9394, we use natural logarithms in this paper and give response values as spectral acceleration in g, for consistency with the other papers in this special issue.

DATA

Ground-Motion Data

The set of data on which the BJF9394 equations are based was chosen from the data used in JB8182 combined with recordings of the 1989 Loma Prieta, the 1992 Petrolia, and the 1992 Landers' earthquakes. Most of the data were collected by the California Division of Mines and Geology's Strong-Motion Instrumentation Program and the U.S. Geological Survey's National Strong-Motion Program. The data set was restricted to shallow earthquakes in western North America with moment magnitude greater than 5.0, shallow earthquakes being defined as those for which the fault rupture lies mainly above a depth of 20 km.

As in JB8182, the BJF9394 studies used values for peak acceleration scaled directly from accelerograms, rather than the processed, instrument-corrected values. We did this to avoid bias in the peak values from the sparsely sampled older data (e.g., Figure 5 in Boore and Joyner, 1982). This bias is not such a problem with the more densely sampled recent data. With a few exceptions we used response spectra as provided by relevant agencies; the exceptions are the data collected by Southern California Edison Company and by S. Hough of the U.S. Geological Survey, for which we computed response spectra ourselves.

The regression analysis for response spectra was done on pseudovelocity response, which is computed by multiplying the relative displacement response by the factor $2\pi/T$, where T is the undamped natural period of the oscillator (the pseudovelocity response spectra provided by the U.S. Geological Survey for the 1979 Coyote lake, the 1979 Imperial Valley, and the 1979 Loma Prieta earthquakes, and perhaps other earthquakes as well, used the damped period, but in the worst case [20 percent damping] this amounts to a difference in response spectra of only 2 percent). In this paper, for consistency with other papers in the issue, the final equations were converted to give pseudoacceleration response in g, where pseudoacceleration response is computed by multiplying the relative displacement response by the factor $(2\pi/T)^2$.

As in JB8182, to avoid bias due to soil-structure interaction, the BJF9394 studies did not use data from structures

three stories or higher, from dam abutments, or from the base of bridge columns. In addition, we included no more than 1 station with the same site condition within a circle of radius 1 km. In such cases, we generally chose the station with the lowest database code number and excluded the others. The radius of 1 km is a somewhat arbitrary choice.

When a strong-motion instrument is triggered by the S wave, the strongest motion may be missed. Unlike in JB8182, the BJF9394 studies made a systematic effort to exclude records from instruments triggered by the S wave (some such records with very emergent S waveforms may have slipped through, but records with emergent S waveforms would capture the peak values of acceleration and spectral response even if they were triggered on S).

A strong-motion data set will be biased by any circumstance that causes values of ground motion to be excluded because they are low, as happens when the ground motion is too weak to trigger the strong-motion instrument, when the ground motion is so weak that an instrument triggers on the S wave, or when records are not digitized because their amplitude is low. To avoid a bias toward larger values, in BJF9394 we imposed a distance cutoff for each earthquake, beyond which we ignored any data available for that earthquake. This cutoff should logically be a function of geologic condition and trigger level of the recording instrument. We ignored geologic condition in the determination of cutoff distance, but we have partially considered the effect of trigger level by distinguishing between those stations employing a trigger sensitive to horizontal motion and those that were triggered on the vertical component of motion. Potentially, every earthquake could have two cutoff distances, depending on the type of trigger used in the recorder. In fact, this was only necessary for the 1971 San Fernando earthquake, which occurred during the time of transition between older instruments that trigger on horizontal motion and newer instruments that employ vertical triggers. For peak acceleration, the cutoff distance is equal to the lesser of the distance to the first record triggered by the S wave and the closest distance to an operational nontriggered instrument. For response spectra we chose to presume that amplitude is a factor in deciding which records are digitized, and we set the cutoff distance to the least of three distances: the distance to the first digitized record triggered by the S wave, the distance to the closest non-digitized recording, or the closest distance to an operational nontriggered instrument. In Table 1, which gives the cutoff distances, the greater-than sign indicates that the cutoff distance is at an unknown distance greater than that indicated. For the 1992 Landers earthquake the digitizing of the analog records was not complete when we assembled the data set for BJF93 and few records from digital instruments had been released. When additional data from the Landers earthquake are added to the data set the cutoff distance for response spectra for that earthquake will probably increase.

In JB8182 we ignored the possible errors introduced by including records triggered by the S wave. Using the cutoff

TABLE 1A.
Cutoff distances for peak acceleration

EQ#	Year	Name	Cutoff Dist. (km)
	1940	Imperial Valley	>12.0
	1952	Kern County	148.0
	1957	Daly City	>8.0
	1966	Parkfield	63.6
	1968	Borrego Mt.	105.0
	1970	Lytle Creek	13.0
	1971	San Fernando	20.2 for H trigger; >60.7 for V trigger
72	1972	Bear Valley	31.0
76	1972	Sitka	145.0
79	1972	Managua	>5.0
84	1973	Pt. Mugu	50.0
97	1974	Hollister	>17.0
109	1975	Oroville	8.0
137	1978	Santa Barbara	>14.0
144	1979	St. Elias	>25.4
146	1979	Coyote Lake	43.0
147	1979	Imperial Valley	64.0
153	1980	Livermore Valley 1	>40.3
154	1980	Livermore Valley 2	>48.3
155	1980	Horse Canyon	47.7
328	1989	Loma Prieta	80.9
349	1992	Petrolia	45.3
352	1992	Landers	119.9

distances shown in Table 1 resulted in the elimination of 56 records from the peak acceleration data and 19 records from the response spectral data set, a significant fraction of the data used in JB8182. In addition, 7 records were deleted for other reasons: information was available only for one horizontal component, the record was obtained on a dam abutment, or available information indicated that the site was underlain by muskeg or peat (records for which only a single horizontal component was available were not deleted if the other component was not operational). BJF93 gives a listing of the records used in the original study that were eliminated from the current analysis.

Because of the relatively low sampling rate of the older data (unevenly sampled, but usually interpolated to 50 samples/sec), the response spectra are not well determined at periods less than 0.1 sec. At longer periods, low signal-to-noise ratios and low-cut filters employed in the processing limit the generally useful band to periods less than about 2 to 4 sec (we hope to extend this range in the future by reprocessing the data). BJF9394 used response spectra for periods between 0.1 and 2 sec.

TABLE 1B.
Cutoff Distances Used for Response Spectra

EQ#	Year	Name	Cutoff Dist. (km)
	1940	Imperial Valley	>12.0
	1952	Kern County	148.0
	1957	Daly City	>8.0
	1966	Parkfield	63.6
	1968	Borrego Mt.	105.0
	1970	Lytle Creek	13.0
	1971	San Fernando	20.2 for H trigger, >60.7 for V trigger
76	1972	Sitka	145.0
79	1972	Managua	>5.0
144	1979	St. Elias	>25.4
146	1979	Coyote Lake	43.0
147	1979	Imperial Valley	64.0
328	1989	Loma Prieta	68.7
349	1992	Petrolia	45.3
352	1992	Landers	65.4

The recording of the 1992 Petrolia earthquake at the Cape Mendocino station provided only lower bounds for the peak acceleration, and therefore the recording was not used for peak acceleration. According to numerical experiments mentioned by Shakal *et al.* (1992a), the high-frequency character of the acceleration trace associated with the peak motion makes the displacement and velocity records insensitive to the actual value of the peak motion. For this reason, BJF9394 used response spectra determined from the recording for periods greater than 0.1 sec.

Predictor Variables

We use moment magnitude as the measure of earthquake size and a distance equal to the closest horizontal distance from the station to a point on the earth's surface that lies directly above the rupture (r_h). We estimated the moment magnitudes and the areas of the rupture surface from a literature review of various published studies for each earthquake. Table 2 gives the rake angles for the earthquakes in the data set, using the convention of Aki and Richards (1980) that reverse slip earthquakes have positive rake angles and the absolute value of the rake for left-lateral slip is less than 90 degrees. We define strike-slip earthquakes as those with a rake angle within 30 degrees of horizontal. All of the earthquakes in the data set are either strike-slip or reverse-slip except for the Daly City earthquake, which appears to be normal-slip (Marsden *et al.*, 1995; Mary Lou Zoback, written communication, 1996). With only one normal-slip earthquake in the data set we do not attempt to include normal-slip earthquakes in our equations for estimating ground motion. Readers interested in estimating ground motion for

TABLE 2.
Rake angles

Quake_Code	Date	Name	Rake	Reference
8		Imperial Valley		Richter (1958)
18		Kern County		Dunbar <i>et al.</i> (1980), Stein and Thatcher (1981)
32		Daly City		Marsden <i>et al.</i> (1995), Mary Lou Zoback (written commun., 1996)
50		Parkfield		McEvilly (1966)
58		Borrego Mountain		Allen and Nordquist (1972)
64		Lytle Creek		L. Jones (oral commun., 1993)
65		San Fernando		Whitcomb (1971), Langston (1978); Heaton (1982)
76		Sitka		Schell and Ruff (1986)
79		Managua		Algermissen <i>et al.</i> (1974)
84		Point Mugu		Boore and Stierman (1976)
97		Hollister		Lee (1974)
137		Santa Barbara		Corbett and Johnson (1982)
144		St. Elias		Hasegawa <i>et al.</i> (1980) and other papers in the same issue
146		Coyote Lake		Liu and Helmberger (1983)
147		Imperial Valley		Archuleta (1984)
153		Livermore Valley		Cockerham <i>et al.</i> (1980)
154		Livermore Valley		Cockerham <i>et al.</i> (1980)
155		Horse Canyon		Given (1983)
328		Loma Prieta		median of values summarized in Table 2 of Wallace <i>et al.</i> (1991)
349		Petrolia		Oppenheimer <i>et al.</i> (1993)
352		Landers		Kanamori <i>et al.</i> (1992)

normal-slip earthquakes should consult Spudich *et al.* (1997, this issue).

Unlike JB8182, the BJF9394 analyses used shear-wave velocity averaged over the upper 30 m as the variable to represent site effects (the value we use is a time-weighted average, computed by dividing 30 m by the S-wave travel time from the surface to 30 m). The regression analysis was first done by BJF93 using a site classification scheme based on the shear-wave velocity averaged over the upper 30 m. This scheme, shown in Table 3, was taken from a classification, based on proposals by Borcherdt (1992, 1994), which was adopted by a Workshop held at the University of Southern California, November 18–20, 1992 to determine site provisions for the National Earthquake Hazard Reduction Reduction Program's (NEHRP) recommended code provisions. The classification was incorporated into the 1994 edition of the NEHRP provisions (BSSC, 1994), but, unfortunately, the letter designations of the classes were changed as shown in Table 4; to avoid confusion in discussing site classes it is necessary to refer specifically to the BJF93 site classes or the NEHRP site classes (BSSC, 1994). In assigning site classifications we used measurements from boreholes at the strong-motion sites where available. Where such measurements were not available we estimated the site classifications by analogy with borehole measurements in similar geologic

TABLE 3.
Definition of Boore *et al.* (1993) site classes

Site Class	Range of Shear Velocities*
	greater than 750 m/s
	360 m/s to 750 m/s
	180 m/s to 360 m/s
	less than 180 m/s

* Shear velocity is averaged over the upper 30 m.

TABLE 4.
Definition of NEHRP site classes (BSSC, 1994)

Site Class	Range of Shear Velocities*
A	greater than 1500 m/sec
B	760 m/sec to 1500 m/sec
C	360 m/sec to 760 m/sec
D	180 m/sec to 360 m/sec
E	less than 180 m/sec

* Shear velocity is averaged over the upper 30 m.

materials; the type of geologic materials underlying each site was obtained in a number of ways: site visits, consultation with geologists familiar with the area, or various geologic maps (in particular, the 1:250,000 scale maps published by the California Division of Mines and Geology; see also Fujinal (1991), who used more detailed maps). Although we expect that some of the site classifications will change as more data become available, we do not anticipate any significant changes in the BJF93 regression coefficients as a result of such changes. Of the four site classes listed in Table 3, class D was poorly represented in the data set and was not included in the analysis.

In BJF93 the site effect was accounted for by determining average amplifications for the motions on BJF93 class B and C sites relative to class A sites (while accounting for differences in distance and magnitude). The residuals (with respect to the motions predicted by BJF93 at class A sites) at those sites for which downhole shear-wave-velocity measurements were available were then used by BJF94a to develop an expression for the site effect directly in terms of the average shear-wave velocity to 30 m.

The earthquake-station pairs and the corresponding predictor variables are given in Tables 5 and 6 for peak acceleration and response spectra, respectively. The information in Tables 5 and 6 is sorted by date, site class, and distance, in that order. The BJF93 site class is given in the column labeled *G*. In addition, Table 5 contains the peak acceleration values (space does not allow a comparable listing of response spectral values). In both tables a borehole number is given if the site classification is based on a nearby borehole. The borehole information is given in BJF93 (with corrections in BJF94a). The distribution in magnitude and distance space is shown in Figure 1, where the data used in JB8182 (but not winnowed out of the current data set) and the data from the three recent earthquakes are plotted with different symbols. It is clear that the recent data fill an important gap in the original data set. It should also be noted that very few data are available for distances beyond about 80 km.

With the equations of BJF93 as the starting point, revisions by BJF94ab led to the development of the equations

summarized in this report. New information has become available regarding the predictor variables for some of the records in the data set. We have determined that the new information would not have a large enough effect on estimated ground motion to justify starting over again and replacing the coefficients of the equations from BJF93 with a new set. We have, however, updated Tables 4 and 5 of BJF93 and Table 5 of BJF94a to reflect the new information; these new tables are Tables 5, 6, and 2, respectively. The data from which the coefficients were originally derived can be found in the tables in BJF93. The first source of new information was a final report by Thiel and Schneider (1993) which superseded a preliminary version that provided average shear-wave velocity data used by BJF93 to assign sites to the different site classes. The average velocity changes produced changes in site class at four sites. Visits in 1994 to sites in the area of the 1992 Petrolia earthquake produced changes in site class at 5 sites. The most significant change involved the magnitude of the 1978 Santa Barbara earthquake, which was assigned a value of 5.1 by BJF93 based on a preliminary moment determination in an abstract by Wallace and Helmberger (1979), which contained a typographical error. The value we now prefer is 5.87, based on number of more recent determinations (Wallace *et al.*, 1981; Ekstrom and Dziewonski, 1985; Bent and Helmberger, 1991). The magnitude value for the Santa Barbara earthquake affects only the equations for peak acceleration not those for response spectra (BJF93 included no response spectral values for the Santa Barbara earthquake, although we probably will in our next study). If the coefficients were revised to accommodate the change, the estimated peak acceleration for linear magnitude scaling would decrease by 11 percent for a magnitude 5.5 reverse-slip earthquake and by lesser amounts for all larger magnitudes and for strike-slip earthquakes. The discrepancy for a magnitude 5.5 earthquake would be 13 percent if quadratic magnitude scaling were introduced. The difference at magnitude 5.5 did not seem large enough to us large justify the introduction of a new set of coefficients, and, as discussed below, we recommend that the equations not be used for magnitudes less than 5.5.

TABLE 5.
Records Used in the Development of the Equations for Peak Acceleration

Date	Earthquake	M	Dist	Station	Lat.	Long.	G	Hole	PA_H1	PA_H2	Reference*
		7.00	12.0	El Centro Array Sta 9	32.794	115.549	C	107	.359	.224	CIT: EERL 76-02
2		7.40	42.0	Taft	35.150	119.460	B	201	.196	.177	CIT: EERL 76-02
2		7.40	85.0	Santa Barbara	34.420	119.700	B	96	.135	.090	CIT: EERL 76-02
2		7.40	109.0	Pasadena - Athenaeum	34.140	118.120	B	92	.054	.048	CIT: EERL 76-02
2		7.40	107.0	Hollywood Storage Bldg PE Lo	34.090	118.340	C	63	.062	.044	CIT: EERL 76-02
		5.30	8.0	San Fran.: Golden Gate Park	37.770	122.480	A	173	.127	.105	CIT: EERL 76-02
		6.10	16.1	Cholame-Shandon: Temblor	35.710	120.170	B	200	.411	.282	CIT: EERL 76-02
		6.10	17.3	Parkfield: Cholame 12W	35.639	120.404	B		.072	.066	CIT: EERL 76-02
		6.10	6.6	Parkfield: Cholame 2	35.733	120.288	C	228	.509		CIT: EERL 76-02
		6.10	9.3	Parkfield: Cholame 5W	35.697	120.328	C	197	.467	.403	CIT: EERL 76-02
		6.10	13.0	Parkfield: Cholame 8W	35.671	120.359	C	198	.279	.276	CIT: EERL 76-02

TABLE 5. (Continued)
Records Used in the Development of the Equations for Peak Acceleration

Date	Earthquake	M	Dist	Station	Lat.	Long.	G	Hole	PA_H1	PA_H2	Reference*
9-Apr-68	Borrego Mount	6.60	45.0	El Centro Array Sta 9	32.794	115.549	C	107	.142	.061	CIT: EERL 76-02
9-Feb-71	San Fernando	6.60	17.0	Lake Hughes Sta 12	34.570	118.560	B	86	.374	.288	CIT: EERL 76-02
9-Feb-71	San Fernando	6.60	25.7	Pasadena - Athenaeum	34.140	118.120	B	92	.114	.103	CIT: EERL 76-02
9-Feb-71	San Fernando	6.60	60.7	Wrightwood	34.360	117.630	B	88	.057	.047	CIT: EERL 76-02
9-Feb-71	San Fernando	6.60	19.6	Lake Hughes Sta 4	34.650	118.478	C	71	.200	.159	CIT: EERL 76-02
30-Jul-72	Sitka	7.70	45.0	Sitka	57.060	135.320	A		.110	.090	USDC: USEQ72
23-Dec-72	Managua	6.20	5.0	Managua: ESSO Refinery	12.145	86.322	C		.390	.330	USGS: Circ. 713
21-Feb-73	Point Mugu	5.60	16.0	Port Hueneme	34.145	119.206	C		.130	.080	USGS: Circ. 713
28-Nov-74	Hollister	5.20	17.0	Hollister - Sago Vault	36.765	121.446	A		.011	.008	USGS: Brady
28-Nov-74	Hollister	5.20	8.0	San Juan Bautista	36.846	121.536	B		.120	.050	USGS: Circ. 717-A
28-Nov-74	Hollister	5.20	10.0	Gavilon College Geol Bldg	36.973	121.568	B		.140	.100	USGS: Circ. 717-A
28-Nov-74	Hollister	5.20	10.0	Hollister City Hall	36.850	121.400	C		.170	.100	USGS: Circ. 717-A
13-Aug-78	Santa Barbara	5.87	0.0	Santa Barbara	34.420	119.700	B	96	.210	.100	CDMG: OSMS PR 22
13-Aug-78	Santa Barbara	5.87	11.0	UCSB: Physical Plant	34.422	119.851	B		.390	.240	CDMG: OSMS PR 22
13-Aug-78	Santa Barbara	5.87	14.0	Goleta Substation	34.470	119.890	B		.280	.240	CDMG: OSMS PR 22
28-Feb-79	St. Elias	7.60	25.4	Icy Bay	59.968	141.643	B		.160	.110	USGS: Circ. 818-A
6-Aug-79	Coyote Lake	5.80	9.1	Gilroy Array 1	36.973	121.572	A	192	.127	.100	USGS: Circ. 854-C
6-Aug-79	Coyote Lake	5.80	1.2	Gilroy Array 6	37.026	121.484	B	196	.419	.344	USGS: Circ. 854-C
6-Aug-79	Coyote Lake	5.80	17.9	San Juan Bautista	36.846	121.536	B		.110	.090	USGS: OFR 79-385
6-Aug-79	Coyote Lake	5.80	19.2	San Juan Bautista: Overpass	36.862	121.578	B		.120	.080	USGS: OFR 79-385
6-Aug-79	Coyote Lake	5.80	30.0	Halls Valley	37.338	121.714	B		.044	.040	USGS: OFR 79-385
6-Aug-79	Coyote Lake	5.80	3.7	Gilroy Array 4	37.005	121.522	C	195	.257	.236	USGS: Circ. 854-C
6-Aug-79	Coyote Lake	5.80	5.3	Gilroy Array 3	36.987	121.536	C	194	.267	.260	USGS: Circ. 854-C
6-Aug-79	Coyote Lake	5.80	7.4	Gilroy Array 2	36.982	121.556	C	193	.263	.196	USGS: Circ. 854-C
15-Oct-79	Imperial Vall	6.50	14.0	Parachute Test Site	32.929	115.699	B	116	.200	.110	USGS: OFR 79-1654
15-Oct-79	Imperial Vall	6.50	23.5	Cerro Prieto	32.420	115.301	B		.167	.149	USGS: PP 1254
15-Oct-79	Imperial Vall	6.50	26.0	Superstition Mtn	32.955	115.823	B		.210	.120	USGS: OFR 79-1654
15-Oct-79	Imperial Vall	6.50	.5	El Centro: Meloland Overpass	32.773	115.447	C		.320	.300	CDMG: OSMS PR 26
15-Oct-79	Imperial Vall	6.50	.6	El Centro Array Sta 7	32.829	115.504	C	105	.520	.360	USGS: OFR 79-1654
15-Oct-79	Imperial Vall	6.50	1.3	El Centro Array Sta 6	32.839	115.487	C	104	.720	.450	USGS: OFR 79-1654
15-Oct-79	Imperial Vall	6.50	1.4	Aeropuerto	32.651	115.332	C		.316	.240	USGS: PP 1254
15-Oct-79	Imperial Vall	6.50	2.6	Bonds Corner	32.693	115.338	C	97	.810	.660	USGS: OFR 79-1654
15-Oct-79	Imperial Vall	6.50	3.8	El Centro Array Sta 8	32.810	115.530	C	106	.640	.500	USGS: OFR 79-1654
15-Oct-79	Imperial Vall	6.50	4.0	El Centro Array Sta 5	32.855	115.466	C	103	.560	.400	USGS: OFR 79-1654
15-Oct-79	Imperial Vall	6.50	5.1	El Centro: Differential Aria	32.796	115.535	C	112	.510	.370	USGS: OFR 79-1654
15-Oct-79	Imperial Vall	6.50	6.2	El Centro Array Sta 9	32.794	115.549	C	107	.400	.270	USGS: OFR 79-1654
15-Oct-79	Imperial Vall	6.50	6.8	El Centro Array Sta 4	32.864	115.432	C	102	.610	.380	USGS: OFR 79-1654
15-Oct-79	Imperial Vall	6.50	7.5	Holtville	32.812	115.377	C	99	.260	.220	USGS: OFR 79-1654
15-Oct-79	Imperial Vall	6.50	7.6	El Centro: Imp. Cnty Cntr FF	32.793	115.560	C	113	.240	.240	CDMG: OSMS PR 26
15-Oct-79	Imperial Vall	6.50	8.4	Mexicali SAHOP	32.618	115.428	C		.459	.311	USGS: PP 1254
15-Oct-79	Imperial Vall	6.50	8.5	El Centro Array Sta 10	32.780	115.567	C	108	.230	.200	USGS: OFR 79-1654
15-Oct-79	Imperial Vall	6.50	8.5	Brawley	32.991	115.512	C	114	.220	.170	USGS: OFR 79-1654
15-Oct-79	Imperial Vall	6.50	10.6	Calexico	32.669	115.492	C		.280	.220	USGS: OFR 79-1654
15-Oct-79	Imperial Vall	6.50	12.6	El Centro Array Sta 11	32.752	115.594	C	109	.380	.380	USGS: OFR 79-1654
15-Oct-79	Imperial Vall	6.50	12.9	Cucapah	32.545	115.235	C		.310		USGS: PP 1254
15-Oct-79	Imperial Vall	6.50	15.0	Westmorland	33.037	115.623	C	115	.110	.080	CDMG: OSMS PR 26
15-Oct-79	Imperial Vall	6.50	16.0	El Centro Array Sta 2	32.916	115.366	C	100	.430	.330	USGS: OFR 79-1654
15-Oct-79	Imperial Vall	6.50	17.7	Chihuahua	32.484	115.240	C		.267	.263	USGS: PP 1254
15-Oct-79	Imperial Vall	6.50	18.0	El Centro Array Station 12	32.718	115.637	C	110	.150	.110	USGS: A
15-Oct-79	Imperial Vall	6.50	22.0	El Centro Array Sta 1	32.960	115.319	C		.150	.150	USGS: OFR 79-1654
15-Oct-79	Imperial Vall	6.50	22.0	El Centro Array Sta 13	32.709	115.683	C	111	.150	.120	USGS: A
15-Oct-79	Imperial Vall	6.50	23.0	Calipatria	33.130	115.520	C	117	.130	.086	USGS: Porcella
15-Oct-79	Imperial Vall	6.50	23.2	Compuertas	32.572	115.083	C		.188	.149	USGS: PP 1254
15-Oct-79	Imperial Vall	6.50	32.0	Plaster City	32.790	115.860	C		.066	.049	USGS: Porcella
15-Oct-79	Imperial Vall	6.50	32.7	Delta	32.356	115.195	C		.349	.235	USGS: PP 1254
15-Oct-79	Imperial Vall	6.50	36.0	Nilar.d	33.239	115.512	C		.100	.070	CDMG: OSMS PR 26
15-Oct-79	Imperial Vall	6.50	43.5	Victoria	32.289	115.103	C		.163	.122	USGS: PP 1254
15-Oct-79	Imperial Vall	6.50	49.0	Coachella Canal Sta 4	33.360	115.590	C		.140	.110	USGS: OFR 79-1654

TABLE 5. (Continued)
Records Used in the Development of the Equations for Peak Acceleration

Date	Earthquake	M	Dist	Station	Lat.	Long.	G	Hole	PA_H1	PA_H2	Reference*
15-Oct-79	Imperial Vall	6.50	60.0	Ocotillo Wells	33.140	116.130	C		.049	.043	USGS: Porcella
24-Jan-80	Livermore Val	5.80	20.8	Antioch	38.015	121.813	B		.045	.010	USGS+CDMG
24-Jan-80	Livermore Val	5.80	33.1	Mission San Jose	37.530	121.919	B	224	.056	.050	USGS+CDMG
24-Jan-80	Livermore Val	5.80	40.3	APEEL Array Sta 3E	37.657	122.061	B	158	.065	.060	USGS+CDMG
24-Jan-80	Livermore Val	5.80	15.7	San Ramon: Eastman Kodak Bld	37.729	121.928	C		.154	.060	USGS+CDMG
24-Jan-80	Livermore Val	5.80	16.7	San Ramon	37.780	121.980	C		.052	.040	USGS+CDMG
24-Jan-80	Livermore Val	5.80	28.5	Tracy	37.766	121.421	C		.086	.050	USGS+CDMG
27-Jan-80	Livermore Val	5.50	10.1	Morgan Territory Park	37.819	121.795	B		.267	.190	USGS+CDMG
27-Jan-80	Livermore Val	5.50	26.5	Antioch: Contra Loma Park	37.972	121.829	B		.026	.030	USGS+CDMG
27-Jan-80	Livermore Val	5.50	29.0	Mission San Jose	37.530	121.919	B	224	.039		USGS+CDMG
27-Jan-80	Livermore Val	5.50	30.9	Antioch	38.015	121.813	B		.112	.050	USGS+CDMG
27-Jan-80	Livermore Val	5.50	37.8	APEEL Array Sta 3E	37.657	122.061	B	158	.065	.040	USGS+CDMG
27-Jan-80	Livermore Val	5.50	4.0	Livermore: Fagundes Ranch	37.753	121.772	C		.259	.220	USGS+CDMG
27-Jan-80	Livermore Val	5.50	17.7	San Ramon: Eastman Kodak Bld	37.729	121.928	C		.275	.090	USGS+CDMG
27-Jan-80	Livermore Val	5.50	22.5	San Ramon	37.780	121.980	C		.058	.040	USGS+CDMG
27-Jan-80	Livermore Val	5.50	48.3	Oakland: 2-Story Office Bldg	37.806	122.267	C	133	.026	.020	USGS+CDMG
25-Feb-80	Horse Canyon	5.30	5.8	Terwilliger Valley: Snodgras	33.480	116.590	A		.123	.088	USGS: Circ. 854-B
25-Feb-80	Horse Canyon	5.30	12.0	Pinyon Flat Observatory	33.607	116.453	A		.133	.118	USGS: Circ. 854-B
25-Feb-80	Horse Canyon	5.30	12.1	Anza Fire Station	33.555	116.673	A		.073	.067	USGS: Circ. 854-B
25-Feb-80	Horse Canyon	5.30	36.1	Sage	33.580	116.931	A		.111	.084	USGS: Circ. 854-B
25-Feb-80	Horse Canyon	5.30	20.6	Hurkey Creek Park	33.676	116.680	B		.097	.076	USGS: Circ. 854-B
25-Feb-80	Horse Canyon	5.30	20.6	Rancho de Anza	33.348	116.400	B		.096	.096	USGS: Circ. 854-B
25-Feb-80	Horse Canyon	5.30	25.3	Puerta La Cruz	33.324	116.683	B		.181	.114	USGS: Circ. 854-B
25-Feb-80	Horse Canyon	5.30	36.3	Cranston Forest Sta	33.740	116.840	B		.110	.094	USGS: Circ. 854-B
25-Feb-80	Horse Canyon	5.30	41.4	Borrego Springs: Air Ranch	33.190	116.280	B		.040	.032	USGS: Circ. 854-B
25-Feb-80	Horse Canyon	5.30	43.6	San Jacinto: Soboda	33.797	116.880	B		.047	.044	USGS: Circ. 854-B
25-Feb-80	Horse Canyon	5.30	44.4	N. Palm Sprngs: P. O.	33.920	116.540	B		.022	.017	USGS: Circ. 854-B
25-Feb-80	Horse Canyon	5.30	35.9	Thousand Palms	33.817	116.390	C		.082	.050	USGS: Circ. 854-B
25-Feb-80	Horse Canyon	5.30	38.5	Indio: So. Calif Gas Co.	33.747	116.214	C		.094	.060	USGS: Circ. 854-B
25-Feb-80	Horse Canyon	5.30	46.1	Hemet City Library	33.748	116.966	C		.057	.046	USGS: Circ. 854-B
25-Feb-80	Horse Canyon	5.30	47.1	San Jacinto	33.784	116.948	C		.080	.062	USGS: Circ. 854-B
18-Oct-89	Loma Prieta	6.92	10.5	Gilroy Array 1	36.973	121.572	A	192	.500	.430	CDMG: OSMS 89-06
18-Oct-89	Loma Prieta	6.92	29.9	Hollister - Sago Vault	36.765	121.446	A		.060	.040	USGS: OFR 89-568
18-Oct-89	Loma Prieta	6.92	32.5	Cherry Flat Reservoir	37.396	121.756	A		.090	.070	USGS: OFR 89-568
18-Oct-89	Loma Prieta	6.92	42.7	Monterey City Hall	36.597	121.897	A	209	.070	.070	CDMG: OSMS 89-06
18-Oct-89	Loma Prieta	6.92	67.6	S. San Fran.: Sierra Pt.	37.674	122.388	A	220	.110	.060	CDMG: OSMS 89-06
18-Oct-89	Loma Prieta	6.92	69.0	Bear Valley Sta 7	36.483	121.180	A		.040	.060	USGS: OFR 89-568
18-Oct-89	Loma Prieta	6.92	72.6	San Fran.: Fire Station 17	37.728	122.385	A		.110	.070	USGS: OFR 89-568
18-Oct-89	Loma Prieta	6.92	77.2	Piedmont Jr High Schl	37.823	122.233	A	212	.080	.070	CDMG: OSMS 89-06
18-Oct-89	Loma Prieta	6.92	78.5	San Fran.: Rincon Hill	37.786	122.391	A	213	.090	.080	CDMG: OSMS 89-06
18-Oct-89	Loma Prieta	6.92	79.5	Yerba Buena Island	37.807	122.361	A		.060	.030	CDMG: OSMS 89-06
18-Oct-89	Loma Prieta	6.92	80.5	San Fran.: Pacific Heights	37.790	122.429	A	214	.050	.060	CDMG: OSMS 89-06
18-Oct-89	Loma Prieta	6.92	0.0	Corralitos	37.046	121.803	B	130	.500	.640	CDMG: OSMS 89-06
18-Oct-89	Loma Prieta	6.92	10.9	Gavilon College Geol Bldg	36.973	121.568	B		.370	.330	CDMG: OSMS 89-06
18-Oct-89	Loma Prieta	6.92	11.7	Saratoga	37.255	122.031	B		.340	.530	CDMG: OSMS 89-06
18-Oct-89	Loma Prieta	6.92	12.0	Saratoga: West Valley Coll.	37.262	122.009	B		.330	.260	CDMG: OSMS 89-06
18-Oct-89	Loma Prieta	6.92	12.3	Gilroy: Old Firehouse	37.009	121.569	B		.250	.280	CDMG: OSMS 89-06
18-Oct-89	Loma Prieta	6.92	12.5	Santa Cruz	37.001	122.060	B	225	.440	.470	CDMG: OSMS 89-06
18-Oct-89	Loma Prieta	6.92	13.2	San Jose: Santa Teresa Hills	37.210	121.803	B		.280	.270	CDMG: OSMS 89-06
18-Oct-89	Loma Prieta	6.92	19.9	Gilroy Array 6	37.026	121.484	B	196	.170	.130	CDMG: OSMS 89-06
18-Oct-89	Loma Prieta	6.92	20.0	Anderson Dam: Downstream	37.166	121.628	B	142	.250	.260	USGS: OFR 89-568
18-Oct-89	Loma Prieta	6.92	21.7	Coyote Lake Dam: Downstream	37.124	121.551	B		.190	.170	CDMG: OSMS 89-06
18-Oct-89	Loma Prieta	6.92	34.1	SAGO South A	36.753	121.396	B	211	.070	.070	CDMG: OSMS 89-06
18-Oct-89	Loma Prieta	6.92	36.1	Calaveras Reservoir South	37.452	121.807	B	143	.130	.080	USGS: OFR 89-568
18-Oct-89	Loma Prieta	6.92	38.7	Woodside	37.429	122.258	B	132	.080	.080	CDMG: OSMS 89-06
18-Oct-89	Loma Prieta	6.92	42.0	Mission San Jose	37.530	121.919	B	224	.110	.130	CDMG: OSMS 89-06
18-Oct-89	Loma Prieta	6.92	46.4	APEEL Array Sta 9	37.478	122.321	B	1	.110	.120	USGS: OFR 89-568
18-Oct-89	Loma Prieta	6.92	46.5	APEEL Array Sta 7	37.484	122.313	B	164	.090	.160	CDMG: OSMS 89-06

TABLE 5. (Continued)
Records Used in the Development of the Equations for Pe

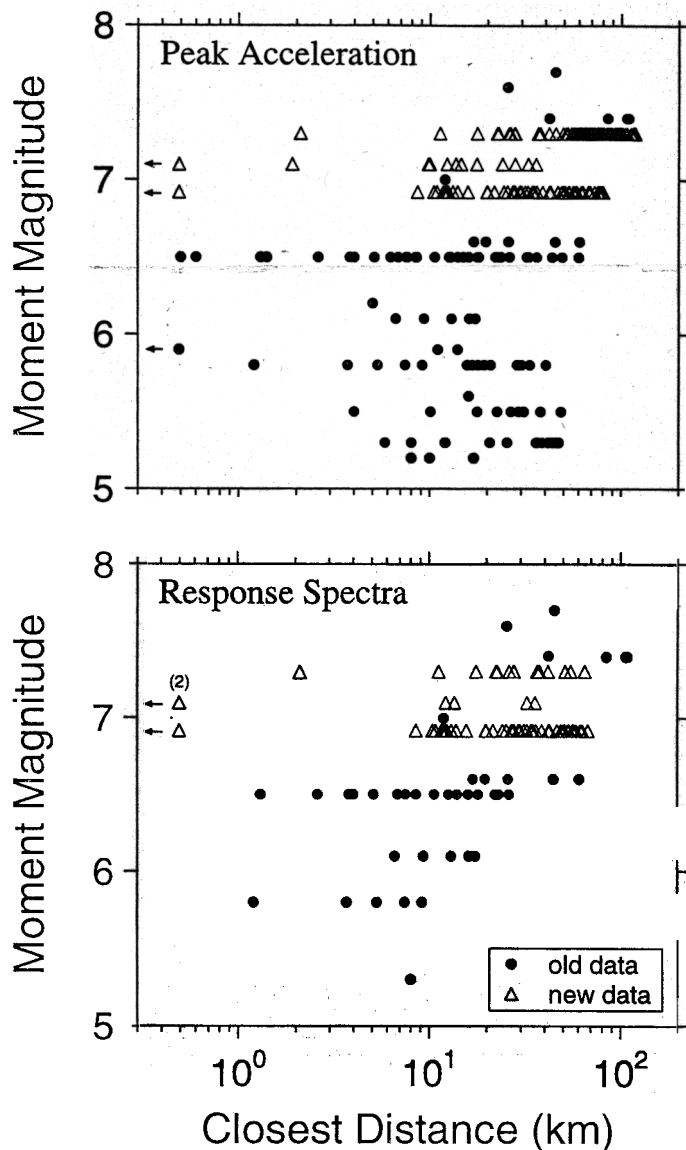
Date	Earthquake	M	Dist	Station	Lat.	Long.	Reference*
18-Oct-89	Loma Prieta	6.92	46.6	APEEL Array Sta 10	37.465	122.343	DMG: OSMS 92-07
18-Oct-89	Loma Prieta	6.92	48.7	Belmont	37.512	122.308	Landslides: OFR 93-557
18-Oct-89	Loma Prieta	6.92	49.9	Sunol Fire Station	37.597	121.880	Gas: OFR 93-557
18-Oct-89	Loma Prieta	6.92	53.0	L. Crystal Spr. Dam: Downstr	37.529	122.361	Earthquake Date: 28-Jun-92
18-Oct-89	Loma Prieta	6.92	53.7	Bear Valley Sta 5	36.673	121.195	28-Jun-92
18-Oct-89	Loma Prieta	6.92	56.0	APEEL Array Sta 3E	37.657	122.061	28-Jun-92
18-Oct-89	Loma Prieta	6.92	57.7	Hayward: BART Station FF	37.670	122.086	28-Jun-92
18-Oct-89	Loma Prieta	6.92	58.7	Hayward City Hall: N. FF	37.679	122.082	28-Jun-92
18-Oct-89	Loma Prieta	6.92	75.9	San Fran.: Diamond Heights	37.740	122.433	28-Jun-92
18-Oct-89	Loma Prieta	6.92	77.6	Big Sur State Park	36.255	121.782	28-Jun-92
18-Oct-89	Loma Prieta	6.92	8.6	Capitola	36.974	121.952	28-Jun-92
18-Oct-89	Loma Prieta	6.92	12.1	Gilroy Array 2	36.982	121.556	28-Jun-92
18-Oct-89	Loma Prieta	6.92	14.0	Gilroy Array 3	36.987	121.536	C 194 .370 .550 CDMG: OSMS 89-06
18-Oct-89	Loma Prieta	6.92	15.8	Gilroy Array 4	37.005	121.522	C 195 .220 .420 CDMG: OSMS 89-06
18-Oct-89	Loma Prieta	6.92	24.3	Gilroy Array 7	37.033	121.434	C 131 .330 .230 CDMG: OSMS 89-06
18-Oct-89	Loma Prieta	6.92	25.4	Hollister: Airport	36.888	121.413	C 147 .290 .270 USGS: OFR 89-568
18-Oct-89	Loma Prieta	6.92	27.0	Agnew	37.397	121.952	C 221 .160 .170 CDMG: OSMS 89-06
18-Oct-89	Loma Prieta	6.92	27.5	Sunnyvale	37.402	122.024	C 136 .220 .190 USGS: OFR 89-568
18-Oct-89	Loma Prieta	6.92	27.8	Hollister: City Hall Annex	36.851	121.402	C .230 .250 USGS: OFR 89-568
18-Oct-89	Loma Prieta	6.92	29.3	Halls Valley	37.338	121.714	C .110 .130 CDMG: OSMS 89-06
18-Oct-89	Loma Prieta	6.92	31.4	Milpitas	37.430	121.897	C .100 .140 CDMG: OSMS 89-06
18-Oct-89	Loma Prieta	6.92	31.4	Salinas	36.671	121.642	C .120 .090 CDMG: OSMS 89-06
18-Oct-89	Loma Prieta	6.92	34.8	Palo Alto: 2-Story Office Bl	37.453	122.112	C 128 .200 .210 CDMG: OSMS 89-06
18-Oct-89	Loma Prieta	6.92	35.0	Stanford: SLAC Test Lab	37.419	122.205	C 134 .290 .190 USGS: OFR 89-568
18-Oct-89	Loma Prieta	6.92	42.4	Fremont	37.535	121.929	C 140 .150 .200 USGS: OFR 89-568
18-Oct-89	Loma Prieta	6.92	50.9	Bear Valley Sta 12	36.658	121.249	C 144 .170 .160 USGS: OFR 89-568
18-Oct-89	Loma Prieta	6.92	56.3	APEEL Array Sta 2E	37.657	122.083	C 150 .140 .180 CDMG: OSMS 89-06
18-Oct-89	Loma Prieta	6.92	61.6	Dublin Fire Station	37.709	121.932	C .080 .090 USGS: OFR 89-568
18-Oct-89	Loma Prieta	6.92	63.2	San Fran.: Airport	37.622	122.398	C 123 .330 .240 CDMG: OSMS 89-06
18-Oct-89	Loma Prieta	6.92	67.3	Bear Valley Sta 10	36.532	121.143	C 146 .100 .130 USGS: OFR 89-568
18-Oct-89	Loma Prieta	6.92	68.8	Livermore: Fagundes Ranch	37.753	121.772	C .040 .040 CDMG: OSMS 89-06
18-Oct-89	Loma Prieta	6.92	75.2	Alameda: Naval Air Station	37.785	122.303	C 119 .260 .200 NCEL: Lew2
18-Oct-89	Loma Prieta	6.92	76.3	Oakland: 2-Story Office Bldg	37.806	122.267	C 133 .200 .260 CDMG: OSMS 89-06
18-Oct-89	Loma Prieta	6.92	78.6	Los Banos	37.106	120.825	C .050 .050 CDMG: OSMS 89-06
18-Oct-89	Loma Prieta	6.92	78.8	Oakland: Outer Harbor Wharf	37.816	122.314	C 122 .290 .270 CDMG: OSMS 89-06
18-Oct-89	Loma Prieta	6.92	80.5	Greenfield	36.321	121.243	C .080 .080 CDMG: OSMS 89-06
25-Apr-92	Petrolia	7.10	1.9	Bunker Hill FAA Site	40.498	124.294	A .210 .180 USGS: Porcella
25-Apr-92	Petrolia	7.10	9.8	Centerville Beach	40.563	124.348	B .480 .320 USGS: Porcella
25-Apr-92	Petrolia	7.10	12.3	Rio Dell	40.503	124.100	B .390 .550 CDMG: OSMS 92-05
25-Apr-92	Petrolia	7.10	13.7	Fortuna: supermarket FF	40.584	124.145	B .120 .120 CDMG: OSMS 92-05
25-Apr-92	Petrolia	7.10	14.6	Fortuna: Fire Station	40.599	124.154	B .280 .320 USGS: Porcella
25-Apr-92	Petrolia	7.10	17.6	Loleta Fire Station	40.644	124.219	B .260 .260 USGS: Porcella
25-Apr-92	Petrolia	7.10	23.9	Coll. of the Redwoods	40.699	124.200	B .180 .140 USGS: Porcella
25-Apr-92	Petrolia	7.10	32.6	Shelter Cove	40.026	124.069	B .180 .240 CDMG: OSMS 92-05
25-Apr-92	Petrolia	7.10	0.0	Petrolia	40.324	124.286	C .690 .620 CDMG: OSMS 92-05
25-Apr-92	Petrolia	7.10	10.0	Ferndale Fire Station	40.576	124.262	C .300 .370 USGS: Porcella
25-Apr-92	Petrolia	7.10	27.8	South Bay Union School	40.735	124.207	C .200 .150 USGS: Porcella
25-Apr-92	Petrolia	7.10	35.8	Eureka: Apartment Bldg FF	40.801	124.148	C .170 .160 CDMG: OSMS 92-05
28-Jun-92	Landers	7.30	2.1	Upper Johnson Valley	34.568	116.612	A .880 .630 SCE
28-Jun-92	Landers	7.30	27.6	Whitewater Cyn	33.989	116.655	A .120 .120 USGS: OFR 93-557
28-Jun-92	Landers	7.30	37.6	Snow Creek	33.888	116.684	A .060 .050 CDMG: OSMS 92-07
28-Jun-92	Landers	7.30	41.9	Twenty-nine Palms	34.021	116.009	A .090 .070 CDMG: OSMS 92-07
28-Jun-92	Landers	7.30	51.3	Silent Valley (Poppet Flat)	33.851	116.852	A .060 .050 CDMG: OSMS 92-07
28-Jun-92	Landers	7.30	56.2	Keenwild	33.707	116.716	A 208 .030 .030 USGS: OFR 93-557
28-Jun-92	Landers	7.30	60.1	Lake Cahuilla	33.628	116.280	A .050 .060 CDMG: OSMS 92-07
28-Jun-92	Landers	7.30	60.8	Pinyon Flat Observatory	33.607	116.453	A .040 .050 USGS: OFR 93-557
28-Jun-92	Landers	7.30	68.2	Tripp Flats	33.602	116.755	A .042 .053 USGS: OFR 93-557
28-Jun-92	Landers	7.30	68.3	Amboy	34.560	115.743	A .150 .120 CDMG: OSMS 92-07

TABLE 6. (Continued)
Records Used in the Development of the Equations for Response Spectra

Date	Earthquake	M	Dist	Station	Lat.	Long.	G	Hole	Source
18-Oct-89		6.92	31.4	Milpitas	37.430	121.897	C		c
18-Oct-89		6.92	31.4	Salinas	36.671	121.642	C		c
18-Oct-89		6.92	34.8	Palo Alto: 2-Story Office Bl	37.453	122.112	C	128	c
18-Oct-89		6.92	35.0	Stanford: SLAC Test Lab	37.419	122.205	C	134	u
18-Oct-89		6.92	42.4	Fremont	37.535	121.929	C	140	u
18-Oct-89		6.92	50.9	Bear Valley Sta 12	36.658	121.249	C	144	u
18-Oct-89		6.92	56.3	APEEL Array Sta 2E	37.657	122.083	C	150	c
18-Oct-89		6.92	61.6	Dublin Fire Station	37.709	121.932	C		u
18-Oct-89		6.92	63.2	San Fran.: Airport	37.622	122.398	C	123	c
18-Oct-89		6.92	67.3	Bear Valley Sta 10	36.532	121.143	C	146	u
25-Apr-92		7.10	0.0	Cape Mendocino	40.348	124.352	A		c
25-Apr-92		7.10	12.3	Rio Dell	40.503	124.100	B		c
25-Apr-92		7.10	13.7	Fortuna: supermarket FF	40.584	124.145	B		
25-Apr-92		7.10	32.6	Shelter Cove	40.026	124.069	B		u
25-Apr-92		7.10	0.0	Petrolia	40.324	124.286	C		c
25-Apr-92		7.10	35.8	Eureka: Apartment Bldg FF	40.801	124.148	C		c
28-Jun-92		7.30	2.1	Upper Johnson Valley	34.568	116.612	A		s
28-Jun-92		7.30	41.9	Twenty-nine Palms	34.021	116.009	A		c
28-Jun-92		7.30	51.3	Silent Valley (Poppet Flat)	33.851	116.852	A		c
28-Jun-92		7.30	11.3	Joshua Tree	34.131	116.314	B		c
28-Jun-92		7.30	17.7	Morongo Valley: MVB	34.049	116.576	B		g
28-Jun-92		7.30	22.5	Desert Hot Springs	33.962	116.509	B		c
28-Jun-92		7.30	22.8	Coolwater Generating Station	34.852	116.858	B		s
28-Jun-92		7.30	27.7	North Palm Springs	33.924	116.547	B		g
28-Jun-92		7.30	27.8	Mission Creek Fault	33.905	116.419	B		g
28-Jun-92		7.30	37.7	Barstow	34.887	117.047	B		c
28-Jun-92		7.30	65.0	Fort Irwin	35.268	116.684	B		c
28-Jun-92		7.30	26.3	Yermo	34.903	116.823	C		c
28-Jun-92		7.30	36.7	Palm Springs	33.829	116.501	C		c
28-Jun-92		7.30	54.9	Indio - Coachella Canal	33.717	116.156	C		c

* References in the Source column are as follows:

- c: Response spectra from the California Strong-Motion Instrumentation Program.
- g: Response spectra computed from digital uncorrected acceleration time series recorded on temporary deployments of GEOS instruments; data provided by S. Hough.
- n: Response spectra from tapes distributed by the World Data Center A for Solid Earth Geophysics, National Geophysical Data Center, Boulder, Colorado; primary data providers are the U.S. Geological Survey and the California Strong-Motion Instrumentation Program.
- s: Response spectra computed from digital uncorrected acceleration time series provided by Dennis Ostrom of the Southern California Edison Company.
- u: Response spectra from U. S. Geological Survey computer files, provided by P. Mork.



▲ **Figure 1.** The distribution of the data in magnitude and distance (each point represents a recording). The data points labeled old data are the ones that were also used in JB8182. The top frame is for the peak acceleration data set, and the bottom is for the response spectral data set.

METHOD

The ground-motion estimation equation is

$$\ln Y = b_1 + b_2(M - 6) + b_3(M - 6)^2 + b_5 \ln r + b_V \ln \frac{V_S}{V_A} \quad (1)$$

where

$$r_{jb} = \sqrt{r_j^2 + h^2} \quad (2)$$

and

$$b_1 = \begin{cases} b_{1SS} & \text{for strike-slip earthquakes;} \\ b_{1RS} & \text{for reverse-slip earthquakes;} \\ b_{1ALL} & \text{if mechanism is not specified.} \end{cases} \quad (3)$$

In this equation Y is the ground-motion parameter (peak horizontal acceleration or pseudoacceleration response in g); the predictor variables are moment magnitude (M), distance (r_{jb} , in km), and average shear-wave velocity to 30 m (V_S , in m/sec). Coefficients to be determined are b_{1SS} , b_{1RS} , b_{1ALL} , b_2 , b_3 , b_5 , h , b_V and V_A . Note that h is a fictitious depth that is determined by the regression.

The coefficients in the equations for predicting ground motion were determined using a weighted, two-stage regres-

sion procedure (Joyner and Boore, 1993, 1994). In the first stage, the distance and site-condition dependence were determined along with a set of amplitude factors, one for each earthquake. In the second stage, the amplitude factors were regressed against magnitude to determine the magnitude dependence.

In a departure from Joyner and Boore (1993) the sum of square errors in the first stage was minimized with respect to the parameter b by a simple numerical search (using the routine GOLDEN [Press *et al.*, 1992]) rather than by linearization. The second-stage regression used a weighting matrix with zero off-diagonal terms (equation (34) in Joyner and Boore, 1993); the value of σ_e was determined by minimizing the square of the difference between the left and right sides of equation (33) in Joyner and Boore (1993).

We tried replacing the term $b_3 \ln r$, which can be thought of as representing geometrical spreading for a simple point source, with $b_4 r - \ln r$ (this would correspond to simple $1/r$ spreading in addition to anelastic attenuation). Doing so, however, led to values of b_4 greater than zero. This result tells us that the motions attenuate less rapidly than $1/r$, at least at distances within 100 km, perhaps because of the effect of critical-angle reflections from layers within and at the base of the crust. Positive values of b_4 in such an expression lead to unreasonable behavior at large distances, so we changed to the form in equation (1).

When the two-stage regression was run by BJF93, fault mechanisms were not differentiated and the site effect was represented by average values for BJF93 classes B and C (with class A as reference). In the first revision of the resulting equations (BJF94a) we took residuals with respect to the equations (for reference class A) at sites where shear velocity had been measured downhole and used the residuals to determine b_V and V_A in equation (1). In the second revision (BJF94b) we took residuals with respect to the BJF93 equations for strike-slip earthquakes and reverse-slip earthquakes and used the residuals to determine the parameters b_{1SS} and b_{1RS} . In the analysis of residuals for both the first and second revisions the same two-stage regression procedure (Joyner and Boore, 1993, 1994) was used as in the analysis of the original data (details are given in BJF94a). Strictly speaking, the revision taking account of fault mechanism should have been done first and then the revised equations used in doing the revision involving site shear velocity, but we have determined that the results would not differ significantly and thus are not changing the coefficients given by BJF94ab.

The coefficient that controls the shear-velocity dependence of response spectral amplification as determined from the data in Table 6, which came entirely from North America, is compared in Figure 2 with the values obtained by Midorikawa *et al.*, (1994) from data in Japan. Also shown are the coefficients proposed by Borcherdt (1994) for determining short-period and mid-period amplification factors in building codes; these were determined from Fourier amplitude spectra of recordings from the 1989 Loma Prieta earthquake.

The mean plus one sigma value of the natural logarithm of the ground-motion value from equation (1) is $\ln Y + \sigma_{\ln Y}$, where $\sigma_{\ln Y}$ is the square root of the overall variance of the regression, given by

$$\sigma_{\ln Y}^2 = \sigma_e^2 + \sigma_c^2 \quad (4)$$

where σ_e^2 represents the earthquake-to-earthquake component of the variability and is determined in the second stage of the regression, and σ_c^2 represents all other components of variability.

$$\sigma_c^2 = \sigma_1^2 + \sigma_c^2 \quad (5)$$

where σ_1^2 is the variance from the first stage of the regression and σ_c^2 represents the correction needed to give the variance corresponding to the randomly-oriented horizontal component.

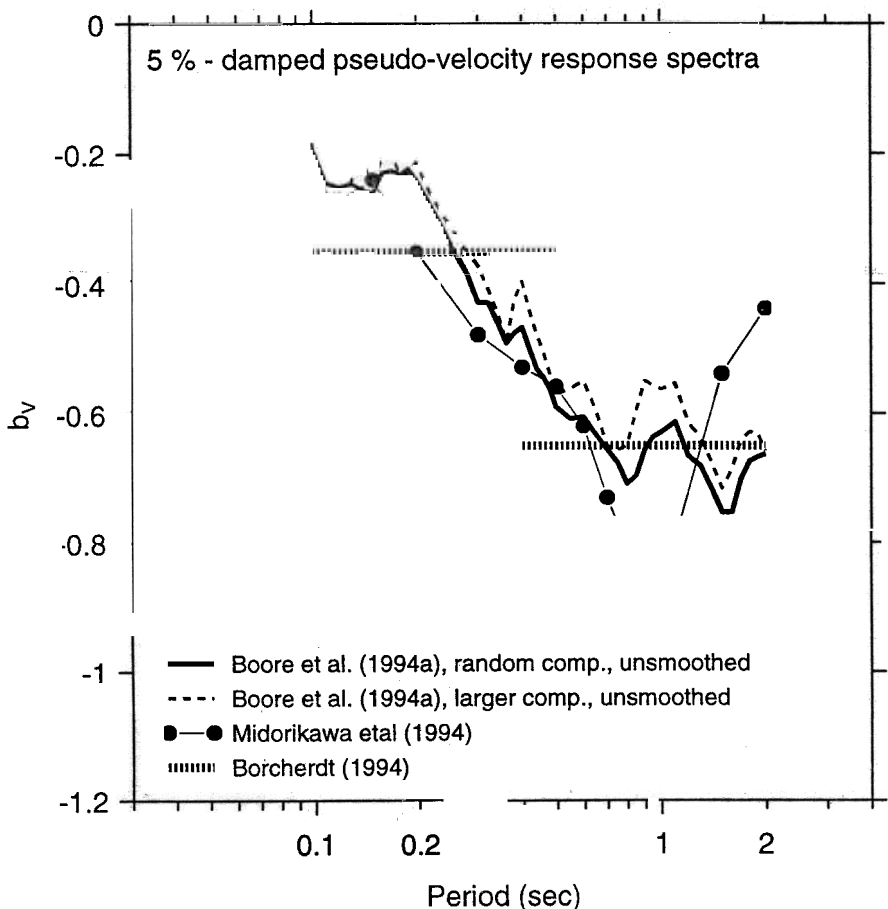
In deriving equations for the randomly-oriented component, we used the geometric mean of the two horizontal-component amplitudes for Y in equation (1) rather than choosing one of the horizontal components randomly. This gives the correct regression coefficients, but the variance σ_1^2 determined by the regression program is reduced below that appropriate for the random horizontal component. To account for the reduction, we computed the variance (σ_c^2) of the horizontal components from the following formula:

$$\sigma_c^2 = \frac{1}{n_{recs}} \sum_{i=1}^{n_{recs}} \frac{(\ln Y_{1j} - \ln Y_{2j})^2}{2} \quad (6)$$

where Y_{ij} is the i th component from the j th recording and the sum is taken over all records for which both horizontal components were available. The few records that did not have both horizontal components were not included in the sum, although they were used in the regression to determine the coefficients in equation (1).

We strongly recommend the use of equation (1) with estimated shear-wave velocity values in preference to the equations of BJF93, which are based on site classes. Values of average shear-wave velocity to be used in equation (1) for estimating ground motions for the NEHRP site classes B, C, and D (BSSC, 1994) and for typical rock and soil sites are given in Table 7. The values given for the NEHRP site classes B, C, and D are simply the geometric means of the velocity values at the boundaries of the site classes. Values are not given for NEHRP classes A and E because they are open-ended. The velocity values for rock and soil come from an analysis by Boore and Joyner (1997) of downhole data illustrated in Figure 3.

The ground-motion prediction equations in this report were obtained with a two-stage maximum-likelihood method. One-stage maximum-likelihood methods have



▲ Figure 2. The coefficient that controls the shear-velocity dependence of response spectral amplification, as determined in BJF94a's analysis of California data and by Midorikawa *et al.* (1994) for data from Japan. Also shown are the coefficients proposed by Borcherdt (1994) for determining short-period and mid-period amplification factors in building codes; these were determined from Fourier amplitude spectra of recordings from the Loma Prieta earthquake.

TABLE 7.
Recommended values of average shear velocity* for use in equation (1)

NEHRP site class B	1070 m/sec
NEHRP site class C	520
NEHRP site class D	250
Rock	620
Soil	310

* Shear velocity is averaged over the upper 30 m.

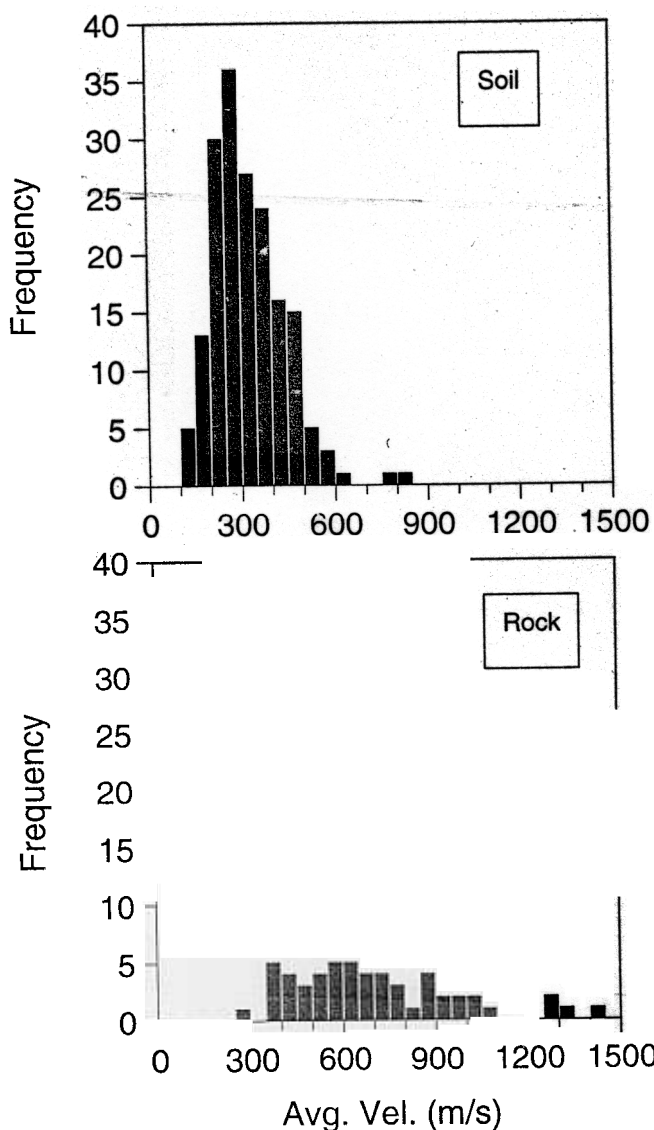
been proposed (for example, Brillinger and Preisler, 1984, 1985; Abrahamson and Youngs, 1992). The one-stage and two-stage methods were compared by BJF94a who, for the one-stage method, used the procedure described in Joyner and Boore (1993), and the results were shown to be very similar.

RESULTS

Equation (1) was fit to the data period-by-period at the 46 periods between 0.1 and 2.0 sec for which the response spectral values had been computed. These periods are distributed in a generally logarithmic manner over the interval.

Plots of the coefficients versus period showed them to have fluctuations that lead to somewhat jagged spectra at a fixed distance and magnitude; the amplitude of the fluctuations is comparable to the uncertainty in the estimated coefficients. Because we wish our equations to produce smooth response spectra, we smoothed the coefficients over period. After some experimentation with various smoothing schemes, we adopted the least-squares fit of a cubic polynomial as the best representation of the smoothed coefficients. Plots comparing smoothed and unsmoothed coefficients are given by BJF93.

Comparisons of response spectra computed from the unsmoothed and the smoothed regression coefficients are given in Figure 4 for a magnitude 7.5 strike-slip earthquake



▲ **Figure 3.** Histograms of shear-wave velocity averaged over the upper 30 m, from downhole surveys in boreholes. Many of the boreholes did not quite reach 30 m, and for the sake of estimating representative velocity distributions, small extrapolations of the travel time to 30 m were used in computing the average velocities. (From Boore and Joyner, 1997.)

at a soil site for distances of 0, 5, 10, 20, 40, and 80 km. Figure 4 illustrates the jaggedness that motivated our smoothing of the coefficients and also demonstrates the effectiveness of the smoothing procedure. Pseudovelocity response spectra (psv) are plotted in the figure even though pseudoacceleration spectra are estimated in equation (1), because pseudovelocity spectra are more convenient for plotting.

Smoothed coefficients for estimating the random horizontal-component pseudoacceleration response by equation (1) are given in Table 8. The coefficients for estimating peak horizontal acceleration are entered in Table 8 as the entries

for zero period. The values of σ_1 , σ_c , σ_r , σ_e , and $\sigma_{\ln Y}$ are the same as those in BJF94b, after correcting for the difference between common and natural logarithms. BJF94a contains coefficients for the larger horizontal-component motions, but only for undifferentiated focal mechanisms. We do not have tables of the larger horizontal-component motions for specified mechanisms.

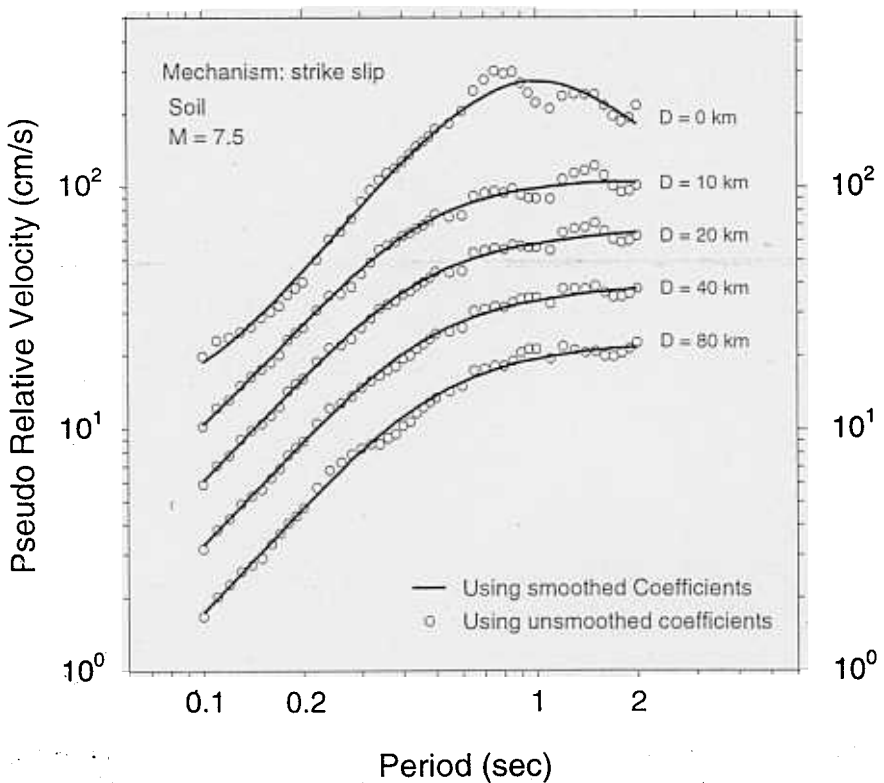
Figures 5, 6, and 7 compare ground-motion estimates from the equations in this report with JB8182. Pseudovelocity response spectra computed from the parameter values in Table 8 are compared in Figure 5 with spectra given by JB82 for magnitude 6.5 and 7.5 earthquakes, mechanism unspecified, at zero distance at a soil site. Our results at zero distance appear to be relatively stable except in the vicinity of 2 sec period. The difference at 2 sec occurs only at small distance. We have no explanation for the difference, except that it must reflect different data. Since the JB82 data set contained few points at small distance, the addition (or subtraction) of data at small distance can make a relatively large change in the estimates.

A similar comparison is given in Figure 6 for a magnitude 6.5 earthquake, mechanism unspecified, at a distance of 20 km at rock and soil sites. Again, there is relatively good agreement except at short periods where our present work shows amplification at soil sites and our original work did not. We suspect that the Loma Prieta earthquake, which was well recorded over a range of site conditions, is at least partly responsible for the difference in short-period amplification shown by the present work.

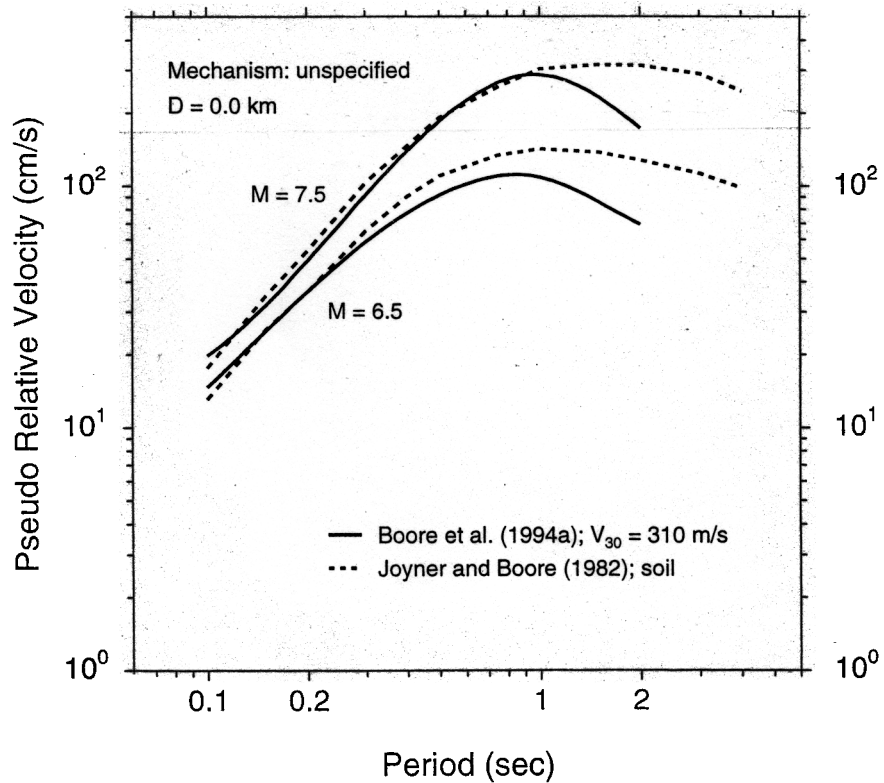
Curves of peak acceleration with distance computed from the parameter values in Table 8 are compared in Figure 7 with curves given by JB82 for magnitude 6.5 and 7.5 earthquakes, mechanism unspecified, at a soil site. The two sets of curves are similar at small distances but the new curves are a factor of two higher than the old curves at 70 km. Comparison of response spectral curves shows the same pattern. In order to understand the reasons for the higher values at large distances we performed a series of analyses of response spectra starting with the old data set. The results showed that both the winnowing of the old data set (which included the elimination of the records that triggered on the S wave) and including the new data from the three recent earthquakes contributed to increasing the values for large distances. (The reasons given in BJF93 for the higher values at large distances were not all valid, as we discovered in reexamining our earlier results.)

Although not shown in the figures, the variance of the ground motions predicted using the results of BJF93/94 has been reduced compared to predictions using JB8182. A series of analyses starting with the old data set showed that the primary cause of the reduction in variance was the winnowing of the data set. The use of weighted regression for the second stage also contributed to the reduction.

The equations in BJF94b (given in Table 8) allow for the effect of fault mechanism. The effect, which is small, is illustrated in Figure 8, which compares pseudovelocity

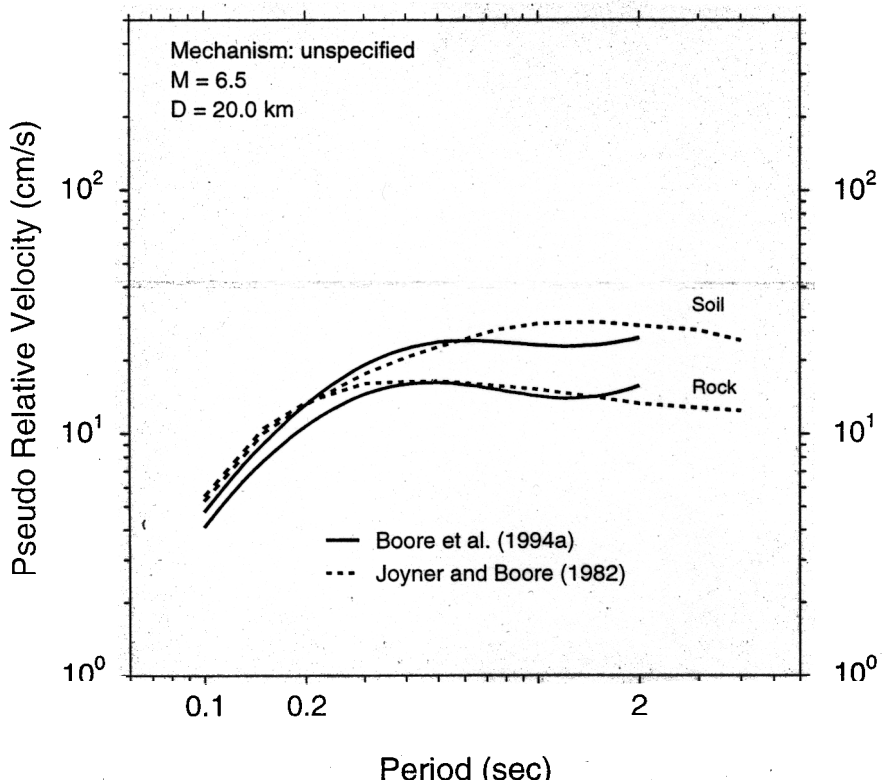


▲ Figure 4. Pseudovelocity response spectra for the random horizontal component at 5 percent damping for a magnitude 7.5 strike-slip earthquake at a soil site, estimated from the unsmoothed and smoothed regression coefficients. The five sets of curves are for distances of 0, 10, 20, 40, and 80 km.

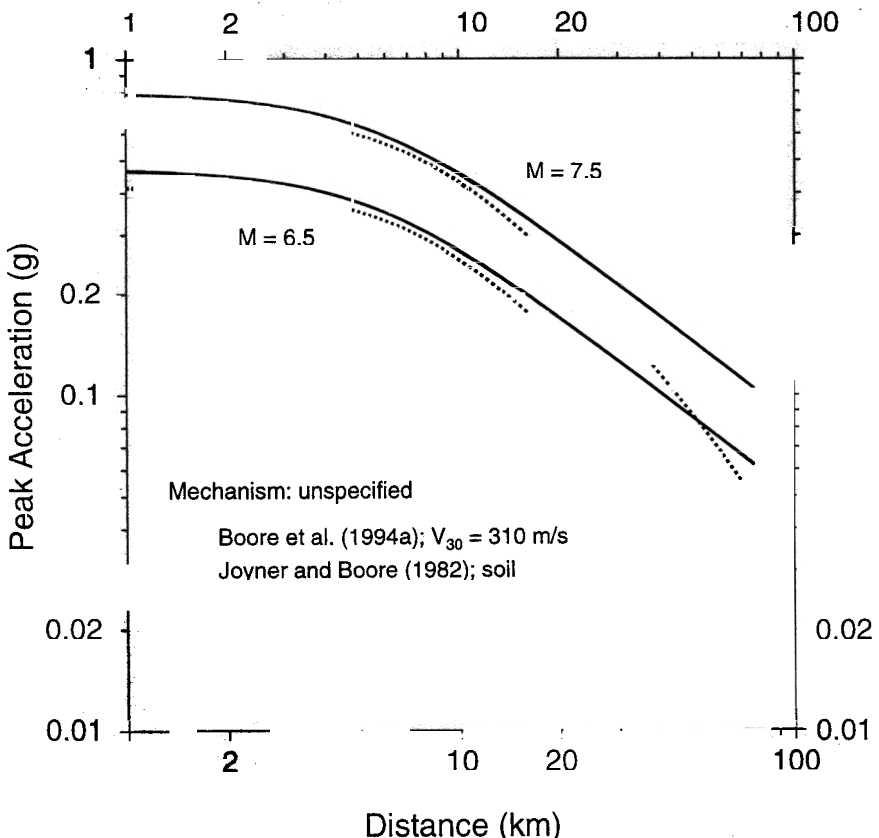


▲ Figure 5. Pseudovelocity response spectra for the random horizontal component at 5 percent damping for magnitude 6.5 and 7.5 earthquakes, mechanism unspecified, at zero distance at a soil site, as given by BJF94a compared with Joyner and Boore (1982).

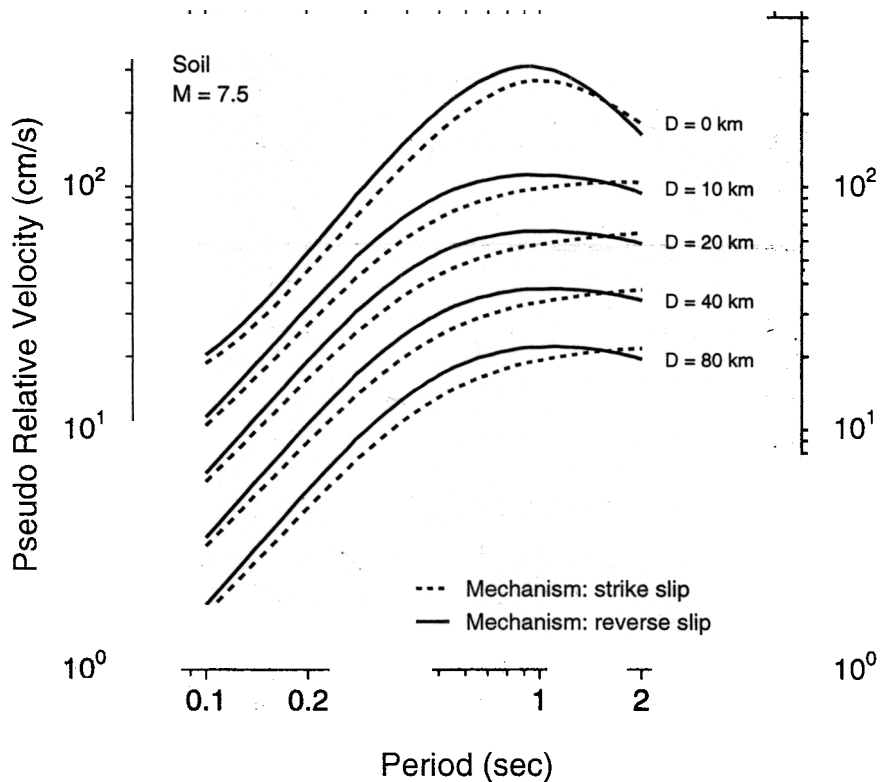
Period	B_{1SS}	B_{1HV}	B_{1ALL}	B_2	B_3	B_5	B_V	V_A	h	σ_1	σ_c	σ_r	σ_e	$\sigma_{ln\gamma}$
0.000	-0.313	-0.117	-0.242	0.527	0.000	-0.778	-0.371	1396.	5.57	0.431	0.226	0.486	0.184	0.520
0.100	1.006	1.087	1.059	0.753	-0.226	-0.934	-0.212	1112.	6.27	0.440	0.189	0.479	0.000	0.479
0.110	1.072	1.164	1.130	0.732	-0.230	-0.937	-0.211	1291.	6.65	0.437	0.200	0.481	0.000	0.481
0.120	1.109	1.215	1.174	0.721	-0.233	-0.939	-0.215	1452.	6.91	0.437	0.210	0.485	0.000	0.485
0.130	1.128	1.246	1.200	0.711	-0.233	-0.939	-0.221	1596.	7.08	0.435	0.216	0.486	0.000	0.486
0.140	1.135	1.261	1.208	0.707	-0.230	-0.938	-0.228	1718.	7.18	0.435	0.223	0.489	0.000	0.489
0.150	1.128	1.264	1.204	0.702	-0.228	-0.937	-0.238	1820.	7.23	0.435	0.230	0.492	0.000	0.492
0.160	1.112	1.257	1.192	0.702	-0.226	-0.935	-0.248	1910.	7.24	0.435	0.235	0.495	0.000	0.495
0.170	1.090	1.242	1.173	0.702	-0.221	-0.933	-0.258	1977.	7.21	0.435	0.239	0.497	0.000	0.497
0.180	1.063	1.222	1.151	0.705	-0.216	-0.930	-0.270	2037.	7.16	0.435	0.244	0.499	0.002	0.499
0.190	1.032	1.198	1.122	0.709	-0.212	-0.927	-0.281	2080.	7.10	0.435	0.249	0.501	0.005	0.501
0.200	0.999	1.170	1.089	0.711	-0.207	-0.924	-0.292	2118.	7.02	0.435	0.251	0.502	0.009	0.502
0.220	0.925	1.104	1.019	0.721	-0.198	-0.918	-0.315	2158.	6.83	0.437	0.258	0.508	0.016	0.508
0.240	0.847	1.033	0.941	0.732	-0.189	-0.912	-0.338	2178.	6.62	0.437	0.262	0.510	0.025	0.511
0.260	0.764	0.958	0.861	0.744	-0.180	-0.906	-0.360	2173.	6.39	0.437	0.267	0.513	0.032	0.514
0.280	0.681	0.881	0.780	0.758	-0.168	-0.899	-0.381	2158.	6.17	0.440	0.272	0.517	0.039	0.518
0.300	0.598	0.803	0.700	0.769	-0.161	-0.893	-0.401	2133.	5.94	0.440	0.276	0.519	0.048	0.522
0.320	0.518	0.725	0.619	0.783	-0.152	-0.888	-0.420	2104.	5.72	0.442	0.279	0.523	0.055	0.525
0.340	0.439	0.648	0.540	0.794	-0.143	-0.882	-0.438	2070.	5.50	0.444	0.281	0.526	0.064	0.530
0.360	0.361	0.570	0.462	0.806	-0.136	-0.877	-0.456	2032.	5.30	0.444	0.283	0.527	0.071	0.532
0.380	0.286	0.495	0.385	0.820	-0.127	-0.872	-0.472	1995.	5.10	0.447	0.286	0.530	0.078	0.536
0.400	0.212	0.423	0.311	0.831	-0.120	-0.867	-0.487	1954.	4.91	0.447	0.288	0.531	0.085	0.538
0.420	0.140	0.352	0.239	0.840	-0.113	-0.862	-0.502	1919.	4.74	0.449	0.290	0.535	0.092	0.542
0.440	0.073	0.282	0.169	0.852	-0.108	-0.858	-0.516	1884.	4.57	0.449	0.292	0.536	0.099	0.545
0.460	0.005	0.217	0.102	0.863	-0.101	-0.854	-0.529	1849.	4.41	0.451	0.295	0.539	0.104	0.549
0.480	-0.058	0.151	0.036	0.873	-0.097	-0.850	-0.541	1816.	4.26	0.451	0.297	0.540	0.111	0.551
0.500	-0.122	0.087	-0.025	0.884	-0.090	-0.846	-0.553	1782.	4.13	0.454	0.299	0.543	0.115	0.556
0.550	-0.268	-0.063	-0.176	0.907	-0.078	-0.837	-0.579	1710.	3.82	0.456	0.302	0.547	0.129	0.562
0.600	-0.401	-0.203	-0.314	0.928	-0.069	-0.830	-0.602	1644.	3.57	0.458	0.306	0.551	0.143	0.569
0.650	-0.523	-0.331	-0.440	0.946	-0.060	-0.823	-0.622	1592.	3.36	0.461	0.309	0.554	0.154	0.575
0.700	-0.634	-0.452	-0.555	0.962	-0.053	-0.818	-0.639	1545.	3.20	0.463	0.311	0.558	0.166	0.582
0.750	-0.737	-0.562	-0.661	0.979	-0.046	-0.813	-0.653	1507.	3.07	0.465	0.313	0.561	0.175	0.587
0.800	-0.829	-0.666	-0.760	0.992	-0.041	-0.809	-0.666	1476.	2.98	0.467	0.315	0.564	0.184	0.593
0.850	-0.915	-0.761	-0.851	1.006	-0.037	-0.805	-0.676	1452.	2.92	0.467	0.320	0.567	0.191	0.598
0.900	-0.993	-0.848	-0.933	1.018	-0.035	-0.802	-0.685	1432.	2.89	0.470	0.322	0.570	0.200	0.604
0.950	-1.066	-0.932	-1.010	1.027	-0.032	-0.800	-0.692	1416.	2.88	0.472	0.325	0.573	0.207	0.609
1.000	-1.133	-1.009	-1.080	1.036	-0.032	-0.798	-0.698	1406.	2.90	0.474	0.325	0.575	0.214	0.613
1.100	-1.249	-1.145	-1.208	1.052	-0.030	-0.795	-0.706	1396.	2.99	0.477	0.329	0.579	0.226	0.622
1.200	-1.345	-1.265	-1.315	1.064	-0.032	-0.794	-0.710	1400.	3.14	0.479	0.334	0.584	0.235	0.629
1.300	-1.428	-1.370	-1.407	1.073	-0.035	-0.793	-0.711	1416.	3.36	0.481	0.338	0.588	0.244	0.637
1.400	-1.495	-1.460	-1.483	1.080	-0.039	-0.794	-0.709	1442.	3.62	0.484	0.341	0.592	0.251	0.643
1.500	-1.552	-1.538	-1.550	1.085	-0.044	-0.796	-0.704	1479.	3.92	0.486	0.345	0.596	0.256	0.649
1.600	-1.598	-1.608	-1.605	1.087	-0.051	-0.798	-0.697	1524.	4.26	0.488	0.348	0.599	0.262	0.654
1.700	-1.634	-1.668	-1.652	1.089	-0.058	-0.801	-0.689	1581.	4.62	0.490	0.352	0.604	0.267	0.660
1.800	-1.663	-1.718	-1.689	1.087	-0.067	-0.804	-0.679	1644.	5.01	0.493	0.355	0.607	0.269	0.664
1.900	-1.685	-1.763	-1.720	1.087	-0.074	-0.808	-0.667	1714.	5.42	0.493	0.359	0.610	0.274	0.669
2.000	-1.699	-1.801	-1.743	1.085	-0.085	-0.812	-0.655	1795.	5.85	0.495	0.362	0.613	0.276	0.672



▲ Figure 6. Pseudovelocity response spectra for the random horizontal component at 5 percent damping for a magnitude 6.5 earthquake, mechanism unspecified, at a distance of 20 km at rock and soil sites, as given by BJF94a compared with Joyner and Boore (1982).



▲ Figure 7. Curves of peak acceleration versus distance for magnitude 6.5 and 7.5 earthquakes, mechanism unspecified, at a soil site, as given by BJF94a compared with Joyner and Boore (1982).



▲ **Figure 8.** Pseudovelocity response spectra for the random horizontal component at 5 percent damping for magnitude 7.5 strike-slip and reverse slip earthquakes at a soil site, as given by the equations in this report (which are the same as given in BJF94b, except for the conversion to ln and pseudo-acceleration response spectra). The five sets of curves are for distances of 0, 10, 20, 40, and 80 km.

response spectra for strike-slip and reverse-slip earthquakes for magnitude 7.5 at soil sites at distances of 0, 5, 10, 20, 40, and 80 km.

Based on the magnitude and distance distribution shown in Figure 1, we stipulate that our equations not be used to predict motions at distances greater than 80 km or magnitudes less than 5.5 or greater than 7.5. These limits are more restrictive than given by BJF9394.

DISCUSSION

Differences between our Relationships and Others

There are three different ways in which our relationships differ from those of most other authors. The first of these is the choice of distance definition. We use a distance r_{jb} equal to the closest horizontal distance from the station to a point on the earth's surface that lies directly above the rupture, and we do the analysis in terms of

$$= \sqrt{r_{jb}^2 + b^2},$$

where b is determined in the regression. Some authors (*e.g.*, Abrahamson and Silva, this issue) use the closest distance in three dimensions from the station to the rupture. Campbell

(this issue) uses the closest distance to what he calls the "seismogenic rupture," the top of which lies at a depth of 3 km or more. He introduced the concept of seismogenic rupture in recognition of the fact that the earth has less strength at shallow depth and may not be able to sustain the stress necessary for energetic rupture. Our point of view is that since the distribution in depth of source strength is unknown, we are better off using the horizontal source distance in conjunction with an effective depth, chosen to fit the strong-motion data. Our definition of distance leads automatically to higher ground-motion values over the hanging wall of dipping faults than over the footwall, in agreement with the analysis of Somerville and Abrahamson (1995). One potential problem with our definition, however, is that it may lead to overestimates of the ground motion at sites directly over the downdip edges of faults that extend to depths near 20 km (earthquakes that extended to significantly greater depth are excluded from our data set). No simple definition, however, will be free of drawbacks, and, all things considered, we continue to prefer our choice.

The second important difference between our results and others is that our relationships have the same magnitude scaling at all source distances. Most other relationships have smaller magnitude scaling at short distances than at long distances. In BJF94a we examined the question of magnitude

scaling at short distances by Monte Carlo simulation and also by examining the magnitude dependence of residuals to our relationships at distances less than 10 km. Both approaches indicated that the magnitude scaling at short distances is not significantly different statistically from what we found for the whole data set.

The third important difference is that we do the regression analysis of response spectra at each period independently. Some analysts do regression analysis on spectral ordinates normalized by peak acceleration and then multiply the results by the value of peak acceleration given by regression analysis of acceleration data. Abrahamson and Silva (this issue) do a multiple-step regression analysis. Peak acceleration is fit in the first step and some of the parameter values are then fixed for subsequent steps in which response values are fit. Our approach requires that the regression coefficients be smoothed over period, but we consider the smoothing to be beneficial rather than detrimental.

Dependence of Variance on Magnitude and Amplitude

A number of authors have suggested that the variance of peak horizontal acceleration depends on magnitude (e.g., Idriss, 1985, and Youngs *et al.*, 1995, who show that the dependence is statistically significant). Others have suggested that the variance of peak horizontal acceleration depends on the value of peak acceleration (Donovan and Bornstein, 1978; Campbell and Bozorgnia, 1994). We have examined these suggestions for our data both for peak acceleration and response spectra. We summarize the results briefly here; a more complete discussion can be found in BJF94. For peak acceleration we, like Youngs *et al.* (1995), find that $\sigma_{\ln Y}$ decreases with increasing magnitude and we, like they, find that most of the effect appears below magnitude 6.0. (Some of the increase in $\sigma_{\ln Y}$ below magnitude 6.0 in our data may reflect the incorrect magnitude assigned to the 1978 Santa Barbara earthquake.) We also find for peak acceleration, like Campbell and Bozorgnia (1994), that $\sigma_{\ln Y}$ decreases with increasing peak acceleration. Most of the effect for peak acceleration with our data set comes from records with peak values less than 0.1 g. For response spectral values we see no significant dependence of variance on either magnitude or amplitude. The difference between the results for peak acceleration and response spectral values is probably due, at least in part, to the relatively few records in the response spectral data set from earthquakes with magnitude less than 6.0 (1 and 5 records from earthquakes of magnitude 5.3 and 5.8, respectively; see Figure 1) and relatively few low-amplitude records in the response spectral data set.

Contribution of Coefficient Uncertainty to Estimation Error

The quantity $\sigma_{\ln Y}$ in Equation (4) and Table 8 is the standard deviation of the data about the prediction equation and is part of the error of a single estimate. The equation itself subject to error resulting from uncertainties in the coeffi-

cients, and that error represents an additional contribution to the estimation error. To evaluate that contribution we used Monte Carlo simulations (Press *et al.*, 1992). We did the simulations with the equations of BJF93, but the results should also be applicable to the equations of this report. We started with a set of coefficients determined by fitting the observed data. We took the magnitude, distance, and site-condition values from the observed data and used the coefficient set in equation (1) of BJF93 to estimate a mean value of the natural logarithm of the ground motion corresponding to each record in the data set. Using a pseudorandom-number generator, we generated a Gaussian random number with mean zero and standard deviation σ_c for each record and a Gaussian random number with zero mean and standard deviation σ_e for each earthquake. Adding the random numbers to the estimated mean values gave an artificial data set of ground-motion values, which we analyzed by the two-stage method to obtain a set of simulated coefficients; we used 100 simulations and thus obtained 100 sets of simulated coefficients. We then used each set of simulated coefficients to predict peak horizontal acceleration and response spectra at 5 percent damping and each of 8 periods from 0.1 to 2.0 sec at BJF93 Class C sites for $M = 6.5$ and 7.5 at $d = 0$ and 20 km. For each magnitude and distance the mean of the 100 estimates of each measure of ground motion provides a measure of the bias in the method, and the spread in the values is a measure of the uncertainty in the ground motions due to stochastic uncertainty in the regression coefficients. The means of the estimates of ground motion from the sets of simulated coefficients were within 8 percent of the ground-motion values predicted from the set of coefficients determined from the observed data for all of the magnitude, distance, and period combinations (including peak acceleration) and were much closer in most cases. This agreement indicates that there is no bias introduced by the particular distribution of the data set over magnitude, distance, and site condition and no bias introduced by the analysis method. The contribution to prediction error from stochastic uncertainties in the coefficients is measured by the standard deviation of the logarithm of the ground-motion parameters calculated from the simulated data sets. The contribution varies substantially with magnitude, distance, and period. It is largest for $M = 7.5$ at $d = 0$, where it ranges from 19 percent for peak acceleration to 45 percent at 2.0 sec period. The scarcity of data points in the vicinity of $M = 7.5$ and $d = 0$ accounts for the large error contribution. For $M = 6.5$ and $d = 20$, where data are more plentiful the contribution ranges from 9 percent for peak acceleration to 21 percent at 2.0 sec period. For all the magnitude, distance and period combinations the contributions are small compared to the standard error of an individual prediction. (The numbers given in this paragraph differ slightly from those in BJF94a because of an error in an input file for a computer run used as a basis for results cited in BJF94a.)

'IMITATIONS OF THE PRESENT WORK AND ROSPECTS FOR IMPROVEMENT

Few response spectral data below magnitude 6.0

Earthquakes with magnitudes less than 6.0 are poorly represented in the response-spectral data set, which includes only one record from a magnitude 5.3 earthquake and six records from a magnitude 5.8 earthquake. Prediction of ground motion for the smaller earthquakes is less important, of course, but it would be desirable to increase the number of data for small earthquakes. This will be accomplished when we add all the recently recorded earthquakes to the data set.

Effect of site conditions on short-period motion

The equations developed from our current data set show differences between site classes for peak acceleration and for response spectra at all periods, while the original equations showed little or no difference for peak acceleration or for response spectra at periods 0.3 sec and smaller. The change is the result of adding new data, and it is an improvement in the sense that the new data set includes a broader range of site conditions. The particular way in which site conditions affect short-period motions, however, may depend on variables not included in the prediction equations. For example, two sites may have the same average shear velocity over the upper 30 m, but they may be underlain by different thicknesses of attenuating material. For a large enough thickness, the effect of anelastic attenuation on short-period motions may largely offset, or even reverse, the effect of amplification. When we add all the recently-recorded earthquakes to the data set and compile all the available geologic site data, we will try adding a variable representing the thickness of attenuating material to the equations.

Averaging velocity over 30 m

The use of average shear-wave velocity to a depth of 30 m as a variable to characterize site conditions is a choice dictated by the relative unavailability of velocity data for greater depths. The ideal parameter would be average shear-wave velocity to a depth of one-quarter wavelength for the period of interest, as was used by Joyner and Fumal (1984; see also Boore and Joyner, 1991, 1997). By the quarter-wavelength rule, 30 m is the appropriate depth for a period of 0.19 sec for the typical rock site (average velocity 620 m/sec) and for a period of 0.39 sec for the typical soil site (average velocity 310 m/sec). The use of shear-wave velocity averaged over 30 m may work reasonably well for other periods, because it will have a high correlation with the average over other depths. We hope, however, to develop estimates of average shear-wave velocity to greater depths at a sufficient number of sites so that we can ultimately provide ground-motion prediction equations in terms of average shear-wave velocity to a depth of one-quarter wavelength.

Distance limitations

There is greater uncertainty in ground-motion estimates at large distances due to the scarcity of data, probably aggravated by regional difference in wave propagation caused by variations in crustal structure and Q . Uncertainty in estimates for large distances is not as important as for smaller distances, but in some circumstances can still be important. There are very few recordings in our data set for distances greater than 80 km, and we recommend that the equations not be used for greater distances. Such a limitation is inherent in the strong-motion data set as long as it is dominated by conventional triggered instruments. In our future work we hope to extend the range of our predictions to larger distances by using weak-motion data recorded on seismographic networks in combination with stochastic methods (e.g., Hanks and McGuire, 1981; Boore, 1983, 1996) to obtain the attenuation of ground motion with distance and strong-motion data to define the magnitude scaling for short distances. The magnitude scaling at distances beyond about 100 km may be somewhat greater than at closer distances for two reasons: the periods controlling the oscillator response may increase because of anelastic attenuation, and the energy radiated by the earthquake may be spread over a longer duration. An example of the distance-dependence of the magnitude scaling can be seen in Figure 9 of Atkinson and Boore (1990).

Basin-generated surface waves

Surface waves have been recorded by strong-motion instruments at sites in deep sedimentary basins (Hanks, 1975). These waves arrive later than the S body waves and have periods in the general range of 3–10 sec. In some, perhaps most, cases these waves are generated at the margins of the sedimentary basins by conversion from body waves in the high-velocity material bounding the basin (Liu and Heaton, 1984; Vidale and Helmberger, 1988; Frankel *et al.*, 1991). At some sites the largest amplitudes at long periods may be due to surface waves. Surface waves are probably not significant for the periods covered by the equations in the present report (two seconds and less), but they represent an important issue in ground-motion prediction for longer periods.

Effect of distance cutoffs that are independent of geology and azimuth

The limits on the distance range within which our equations may be used for predicting ground motion are made more severe by our attempt to avoid bias due to instruments that do not trigger. To avoid that bias, we exclude from the data set for each earthquake all records obtained at distances equal to or greater than the closest operational instrument that did not trigger or that triggered on the S wave. We use different cutoff distances for stations employing a trigger sensitive to horizontal motion and those with a trigger sensitive to vertical motion, but for simplicity we use cutoff distances independent of geologic site conditions and independent of azimuth. Because amplitude depends on site conditions and on azimuth through the effects of radiation

pattern and directivity, the use of cutoff distances independent of geology and azimuth may result in the unnecessary exclusion of records. We choose simplicity and objectivity, however, over increasing the number of records in the data set, and we believe avoiding bias is far more important than increasing the number of data. Alternative methods of avoiding bias are available that do not require the exclusion of records (Toro, 1981; McLaughlin, 1991). Although these methods add significantly to the complexity of the analysis we may consider these methods in our future work. They will become largely unnecessary, however, if we have functions giving ground-motion distance dependence developed by stochastic methods with the help of data other than strong-motion data, as described above.

ACKNOWLEDGMENTS

We wish to thank Sue Hough and Dennis Ostrom for recordings of the Landers earthquake, and Norm Abrahamson, Allin Cornell, and Robin McGuire for discussions about regression analysis of strong-motion data. We also thank Norm Abrahamson, Ken Campbell, and Chuck Mueller for comments on earlier versions of the paper. We are grateful to Ken Lajoie, Patty McCrory, Bob McLaughlin, Dan Ponti, and John Tinsley for discussions about site geology, and to April Converse Miller, Bob Darragh, Ed Etheredge, and Peter Mork for help with the data set. Julian Bommer helped us with the initial formulation of the database structure. Roger Borcherdt, Kaye Shedlock, Paul Spudich, and an unnamed reviewer provided useful reviews of the paper. This work was partially supported by the U.S. Nuclear Regulatory Commission. ☐

REFERENCES

- Abrahamson, N. A. and R. R. Youngs (1992). A stable algorithm for regression analysis using the random effects model, *Bull. Seism. Soc. Am.*, **82**, 505–510.
- Aki, K. and P. G. Richards (1980). *Quantitative Seismology Theory and Methods* 1, 557 pp., W. H. Freeman and Company.
- Algermissen S. T., J. W. Dewey, C. J. Langer, and W. H. Dillinger (1974). The Managua, Nicaragua, earthquake of December 23, 1972: Location, focal mechanism, and intensity distribution, *Bull. Seism. Soc. Am.*, **64**, 993–1,004.
- Allen, C. R. and J. M. Nordquist (1972). Foreshock, main shock, and larger aftershocks of the Borrego Mountain earthquake, *U.S. Geol. Surv. Prof. Paper* 787, 16–23.
- Archuleta, R. J. (1984). A faulting model for the 1979 Imperial Valley earthquake, *J. Geophys. Res.*, **89**, 4,559–4,585.
- Atkinson, G. M. and D. M. Boore (1990). Recent trends in ground motion and spectral response relations for North America, *Earthquake Spectra*, **6**, 15–35.
- Bent, A. L. and D. V. Helmberger (1991). Seismic characteristics of earthquakes along the offshore extension of the western Transverse Ranges, California, *Bull. Seism. Soc. Am.*, **81**, 399–422.
- Boore, D. M. (1983). Stochastic simulation of high-frequency ground motions based on seismological models of the radiated spectra, *Bull. Seism. Soc. Am.*, **73**, 1,865–1,894.
- Boore, D. M. (1996). SMSIM—Fortran programs for simulating ground motions from earthquakes: Version 1.0, *U.S. Geol. Surv. Open-File Rept.* 96-80-A, 73 pp.
- Boore, D. M. and D. J. Stierman (1976). Source parameters of the Pt. Mugu, California, earthquake of February 21, 1973, *Bull. Seism. Soc. Am.*, **66**, 385–404.
- Boore, D. M. and W. B. Joyner (1982). The empirical prediction of ground motion, *Bull. Seism. Soc. Am.*, **72**, S43–S60.
- Boore, D. M. and W. B. Joyner (1991). Estimation of ground motion at deep-soil sites in eastern North America, *Bull. Seism. Soc. Am.*, **81**, 2,167–2,185.
- Boore, D. M. and W. B. Joyner (1997). Site amplification for generic rock sites, *Bull. Seism. Soc. Am.* (in press).
- Boore, D. M., W. B. Joyner, and T. E. Fumal (1993). Estimation of response spectra and peak accelerations from western North American earthquakes: An interim report, *U.S. Geol. Surv. Open-File Rept.* 93-509, 72 pp.
- Boore, D. M., W. B. Joyner, and T. E. Fumal (1994a). Estimation of response spectra and peak accelerations from western North American earthquakes: An interim report, Part 2, *U.S. Geol. Surv. Open-File Rept.* 94-127, 40 pp.
- Boore, D. M., W. B. Joyner, and T. E. Fumal (1994b). Ground motion estimates for strike- and reverse-slip faults, provided to the Southern California Earthquake Center and widely distributed as an insert in Boore et al. (1994a), 4 pp.
- Borcherdt, R. D. (1992). Simplified site classes and empirical amplification factors for site-dependent code provisions, *Proc. NCEER/SEAOC/BSSC Workshop on Site Response During Earthquakes and Seismic Code Provisions*, Univ. S. California, Los Angeles, California, November 18–20, 1992, in press.
- Borcherdt, R. D. (1994). Estimates of site-dependent response spectra for design (methodology and justification), *Earthquake Spectra*, **10**, 617–653.
- Brillinger, D. R. and H. K. Preisler (1984). An exploratory analysis of the Joyner-Boore attenuation data, *Bull. Seism. Soc. Am.*, **74**, 1,441–1,450.
- Brillinger, D. R. and H. K. Preisler (1985). Further analysis of the Joyner-Boore attenuation data, *Bull. Seism. Soc. Am.*, **75**, 611–614.
- Brune, J.N., F.L. Vernon III, R.S. Simons, J. Prince, and E. Mena (1982). Strong-motion data recorded in Mexico during the main shock, in *The Imperial Valley, California, Earthquake of October 15, 1979*, *U.S. Geol. Surv. Prof. Paper* 1254, 319–349.
- BSSC (1994). NEHRP recommended provisions for seismic regulations for new buildings, Part 1—Provisions, FEMA 222A, Federal Emergency Management Agency, 290 pp.
- California Division of Mines and Geology (1992). Second quick report on CSMIP strong-motion records from the June 28, 1992 earthquakes near Landers and Big Bear, California, *OSMS Report 92-07*, 10 pp.
- California Institute of Technology (1976). Strong motion earthquake accelerograms: Index volume, *Earthquake Engineering Research Lab. Report EERL 76-02*, 72 pp.
- Campbell, K. W. and Y. Bozorgnia (1994). Near-source attenuation of peak horizontal acceleration from worldwide accelerograms recorded from 1957 to 1993, *Proc. Fifth U. S. National Conference on Earthquake Engineering* 3, Chicago, Illinois, July 10–14, 1994, 283–292.
- Cockerham, R. S., F. W. Lester, and W. L. Ellsworth (1980). A preliminary report on the Livermore Valley earthquake sequence January 24–February 26, 1980, *U.S. Geol. Surv. Open-File Rept.* 80-714.
- Corbett, E. J. and C. E. Johnson (1982). The Santa Barbara, California, earthquake of 13 August 1978, *Bull. Seism. Soc. Am.*, **72**, 2,201–2,226.
- Donovan, N. C. and A. E. Bornstein (1978). Uncertainties in seismic risk procedures, *Proc. Am. Soc. Civil Eng., J. Geotech. Eng. Div.*, **104**, 869–887.
- Dunbar, W. S., D. M. Boore, and W. Thatcher (1980). Pre-, co-, and postseismic strain changes associated with the 1952 $M_L = 7.2$ Kern County, California, earthquake, *Bull. Seism. Soc. Am.*, **70**, 1,893–1,905.

- Ekström, G. and A. M. Dziewonski (1985). Centroid-moment tensor solutions for 35 earthquakes in western North America (1977–1983), *Bull. Seism. Soc. Am.*, **75**, 23–39.
- Etheredge, E., R. Maley, R. Porcella, and J. Switzer (1993). Strong-motion accelerograph records from the $M = 7.5$ Landers, California earthquake of June 28, 1992, *U.S. Geol. Surv. Open-File Rept. 93-557*, 216 pp.
- Frankel, A., S. Hough, P. Friberg, and R. Busby (1991). Observations of Loma Prieta aftershocks from a dense array in Sunnyvale, California, *Bull. Seism. Soc. Am.*, **81**, 1,900–1,922.
- Fumal, T.E. (1991). A compilation of the geology and measured and estimated shear-wave velocity profiles at strong-motion stations that recorded the Loma Prieta, California, earthquake, *U.S. Geol. Surv. Open-File Rept. 91-311*.
- Given, D. D. (1983). Seismicity and structure of the trifurcation in the San Jacinto fault zone, southern California, *M.S. thesis, Cal. State University, Los Angeles*, 73 pp.
- Hanks, T. C. (1975). Strong ground motion of the San Fernando, California, earthquake: ground displacements, *Bull. Seism. Soc. Am.*, **65**, 193–225.
- Hanks, T. C. and R. K. McGuire (1981). The character of high frequency strong ground motion, *Bull. Seism. Soc. Am.*, **71**, 2,071–2,095.
- Hasegawa, H. S., J. C. Lahr, and C. D. Stephens (1980). Fault parameters of the St. Elias, Alaska, earthquake of February 28, 1979, *Bull. Seism. Soc. Am.*, **70**, 1,651–1,660.
- Heaton, T. H. (1982). The 1971 San Fernando earthquake: A double event?, *Bull. Seism. Soc. Am.*, **72**, 2,037–2,062.
- Idriss, I. M. (1985). Evaluating seismic risk in engineering practice, *Proc. Eleventh Internat. Conf. on Soil Mech. and Foundation Eng.*, August 12–16, 1985, San Francisco, California, **1**, 255–320, A. A. Balkema, Rotterdam.
- Joyner, W.B. and D.M. Boore (1981). Peak acceleration and velocity from strong-motion records including records from the 1979 Imperial Valley, California, earthquake, *Bull. Seism. Soc. Am.*, **71**, 2,011–2,038.
- Joyner, W.B. and D.M. Boore (1982). Prediction of earthquake response spectra, *U.S. Geol. Surv. Open-File Rept. 82-977*, 16 pp.
- Joyner, W.B. and D.M. Boore (1993). Methods for regression analysis of strong-motion data, *Bull. Seism. Soc. Am.*, **83**, 469–487.
- Joyner, W. B. and D. M. Boore (1994). Errata, *Bull. Seism. Soc. Am.*, **84**, 955–956.
- Joyner, W. B. and T. E. Fumal (1984). Use of measured shear-wave velocity for predicting geologic site effects on strong ground motion, *Proc. Eighth World Conf. on Earthquake Eng. (San Francisco)*, **2**, 777–783.
- Kanamori, H., H. K. Thio, D. Dreger, E. Hauksson, and T. Heaton (1992). Initial investigation of the Landers, California, earthquake of 28 June 1992 using TERRAscope, *Geophys. Res. Lett.*, **19**, 2,267–2,270.
- Langston, C. A. (1978). The February 9, 1971 San Fernando earthquake: A study of source finiteness in teleseismic body waves, *Bull. Seism. Soc. Am.*, **68**, 1–29.
- Lee, W. H. K. (1974). A preliminary study of the Hollister earthquake of November 28, 1974 and its major aftershocks, (unpublished manuscript dated December 6, 1974).
- Lew, T.K. (1990). Earthquake preparedness: An analysis of the 1989 Loma Prieta earthquake and isoseismal maps for selected historic earthquakes in the San Francisco Bay region, *Naval Civil Engineering Lab Technical Memorandum 51-086*, Port Hueneme, California.
- Liu, H.-L. and D. V. Helmberger (1983). The near-source ground motion of the 6 August 1979 Coyote Lake, California, earthquake, *Bull. Seism. Soc. Am.*, **73**, 201–218.
- Liu, H.-L. and T. Heaton (1984). Array analysis of the ground velocities and accelerations from the 1971 San Fernando, California, earthquake, *Bull. Seism. Soc. Am.*, **74**, 1,951–1,968.
- McEvilly, T. V. (1966). Preliminary seismic data June-July, 1966, Monterey and San Luis Obispo Counties, California, preliminary report, *Bull. Seism. Soc. Am.*, **56**, 967–971.
- McJunkin, R.D. and J.T. Ragsdale (1980a). Compilation of strong-motion records and preliminary data from the Imperial Valley earthquake of 15 October 1979, *Calif. Div. Mines and Geology Preliminary Report 26*, 53 pp.
- McJunkin, R.D. and J.T. Ragsdale (1980b). Strong-motion records from the Livermore earthquake of 24 and 26 January 1980, *Calif. Div. Mines and Geology Preliminary Report 2*, 91 pp.
- McLaughlin, K. L. (1991). Maximum likelihood estimation of strong-motion attenuation relationships, *Spectra*, **7**, 267–279.
- Maley, R., A. Acosta, F. Ellis, E. Etheredge, L. Foote, D. Johnson, R. Porcella, M. Salsman, and J. Switzer (1989). U.S. Geological Survey strong-motion records from the northern California (Loma Prieta) earthquake of October 17, 1989, *U.S. Geol. Surv. Open-File Rept. 89-568*, 85 p.
- Marsden, R., M. L. Zoback, D. Dreger, B. Julian, J. Olson, and T. Parsons (1995). M 5.3 normal? faulting event adjacent to the San Andreas fault on the San Francisco Peninsula, *Eos, Trans. Amer. Geophys. Un.*, **76**, F423–F424.
- Midorikawa, S., M. Matsuoka, and K. Sakugawa (1994). Site effects on strong-motion records observed during the 1987 Chiba-Ken-Toho-Oki, Japan earthquake, *Proc. 9th Japan Earthq. Eng. Symp.*, **3**, E085–E090.
- Oppenheimer, D., G. Beroza, G. Carver, L. Dengler, J. Eaton, L. Gee, F. Gonzalez, A. Jayko, W. H. Li, M. Lisowski, M. Magee, G. Marshall, M. Murray, R. McPherson, B. Romanowicz, K. Satake, R. Simpson, P. Somerville, R. Stein, and D. Valentine (1993). The Cape Mendocino, California, earthquakes of April 1992: Subduction at the triple junction, *Science*, **261**, 433–438.
- Porcella, R.L. and R.B. Matthiesen (1979). Preliminary summary of the U.S. Geological Survey strong-motion records from the October 15, 1979 Imperial Valley earthquake, *U.S. Geol. Surv. Open-File Rept. 79-1654*, 41 pp.
- Porcella, R.L. and R.B. Matthiesen, R.D. McJunkin, and J.T. Ragsdale (1979). Compilation of strong-motion records from the August 6, 1979 Coyote Lake earthquake, *U.S. Geol. Surv. Open-File Rept. 79-385* and *Calif. Div. Mines and Geology Preliminary Report 28*, 71 pp.
- Porter, L.D. (1978). Compilation of strong-motion records recovered from the Santa Barbara earthquake of 13 August 1978, *Calif. Div. Mines and Geology Preliminary Report 22*, 43 pp.
- Press, W.H., S.A. Teukolsky, W.T. Vetterling, and B.P. Flannery (1992). *Numerical Recipes in FORTRAN, the Art of Scientific Computing*, 2nd. ed., Cambridge University Press, Cambridge, U.K., 963 pp.
- Richter, C. F. (1958). *Elementary Seismology*, W. H. Freeman and Company, San Francisco, 768 pp.
- Schell, M. M. and L. J. Ruff (1986). Southeastern Alaska tectonics: Source process of the large 1972 Sitka earthquake (abs), *Eos, Trans. Amer. Geophys. Un.*, **67**, 304.
- Shakal, A., M. Huang, M. Reichle, C. Ventura, T. Cao, R. Sherburne, M. Savage, R. Darragh, and C. Peterson (1989). CSMIP strong-motion records from the Santa Cruz Mountains (Loma Prieta) earthquake of 17 October 1989, *Calif. Div. Mines and Geology Report No. OSMS 89-06*, 196 pp.
- Shakal, A., R. Darragh, M. Huang, T. Cao, R. Sherburne, R. Sydnor, P. Malhotra, C. Cramer, J. Wampole, P. Fung, and C. Peterson (1992a). CSMIP strong-motion records from the Petrolia, California earthquakes of April 25–26, 1992, *Calif. Div. Mines and Geology Report No. OSMS 92-05*, 74 pp.
- Shakal, A., M. Huang, T. Cao, R. Sherburne, R. Sydnor, P. Fung, P. Malhotra, C. Cramer, F. Su, R. Darragh, and J. Wampole (1992b). CSMIP strong-motion records from the Landers, California earthquake of 28 June 1992, *Calif. Div. Mines and Geology Report No. OSMS 92-09*, 330 pp.

- Somerville, P. G. and N. A. Abrahamson (1995). Prediction of ground motions for thrust earthquakes, Report to the California Strong Motion Instrumentation Program.
- Spudich, P., J. B. Fletcher, M. Hellweg, J. Boatwright, C. Sullivan, W. B. Joyner, T. C. Hanks, D. M. Boore, A. McGarr, L. M. Baker, and A. G. Lindh (1996). Earthquake ground motions in extensional tectonic regimes, *U.S. Geol. Surv. Open-File Rept.* 96-292, 351 pp.
- Stein, R. S. and W. Thatcher (1981). Seismic and aseismic deformation associated with the 1952 Kern County, California, earthquake and relationship to the Quaternary history of the White Wolf fault, *J. Geophys. Res.*, **86**, 4,913–4,928.
- Thiel, C. C., Jr., and J. F. Schneider (1993). Investigations of thirty-three Loma Prieta earthquake strong motion recording sites, final report of project sponsored by the Building Contractors Society of Japan and the Electric Power Research Institute, California Universities for Research in Earthquake Engineering (CUREE), Dept. of Civil Engineering, Stanford Univ., Stanford, Calif.
- Toro, G. R. (1981). Biases in seismic ground motion prediction, Massachusetts Institute of Technology, *Department of Civil Eng. Res. Rept. R81-22*, Cambridge, Massachusetts, 133 pp.
- U.S. Dept. of Commerce (1974). United States Earthquakes, 1972 (J.L. Coffman and C.A. von Hake, Eds.) 119 pp.
- U.S. Geol. Survey (1974). Seismic engineering program report, *U.S. Geol. Surv. Circular 713*, 19 pp.
- U.S. Geol. Survey (1975). Seismic engineering program report, *U.S. Geol. Surv. Circular 717-A*, 17 pp.
- U.S. Geol. Survey (1979). Seismic engineering program report, *U.S. Geol. Surv. Circular 818-A*, 20 pp.
- U.S. Geol. Survey (1980a). Seismic engineering program report, *U.S. Geol. Surv. Circular 854-B*, 25 pp.
- U.S. Geol. Survey (1980b). Seismic engineering program report, *U.S. Geol. Surv. Circular 854-C*, 19 pp.
- U.S. Geol. Survey (1981). Seismic engineering program report, *U.S. Geol. Surv. Circular 914*, 19 pp.
- Vidale, J. E. and D. V. Helmberger (1988). Elastic finite-difference modeling of the 1971 San Fernando, California, earthquake, *Bull. Seism. Soc. Am.*, **78**, 122–141.
- Wallace, T. C. and D. V. Helmberger (1979). A model of the strong ground motion of the August 13, 1978 Santa Barbara earthquake (abstract), *Eos, Trans. Amer. Geophys. Un.*, **60**, 895.
- Wallace, T. C., D. V. Helmberger, and J. E. Ebel (1981). A broadband study of the 13 August 1978 Santa Barbara earthquake, *Bull. Seism. Soc. Am.*, **71**, 1,701–1,718.
- Wallace, T. C., A. Velasco, J. Zhang, and T. Lay (1991). A broadband seismological investigation of the 1989 Loma Prieta, California, earthquake: Evidence for deep slow slip?, *Bull. Seism. Soc. Am.*, **81**, 1,622–1,646.
- Whitcomb, J. H. (1971). Fault-plane solutions of the February 9, 1971, San Fernando earthquake and some aftershocks, *U.S. Geol. Surv. Prof. Paper 733*, 30–32.
- Youngs, R. R., N. Abrahamson, F. Makdisi, and K. Sadigh (1995). Magnitude-dependent variance of peak ground acceleration, *Bull. Seism. Soc. Am.*, **85**, 1,161–1,176.

*U.S. Geological Survey
 345 Middlefield Road
 Menlo Park, California 94025
 boore@samoa.wr.usgs.gov
 joyner@samoa.wr.usgs.gov
 tfumal@isdmnl.wr.usgs.gov*